

**Innovations Deserving  
Exploratory Analysis Programs**

*Highway IDEA Program*

---

**An Acoustic Emission-Based Test to Determine Asphalt Binder  
and Mixture Embrittlement Temperature**

**Final Report for NCHRP-IDEA Project 144**

*Prepared by:  
William G. Buttlar, Behzad Behnia, Henrique M. Reis  
University of Illinois at Urbana-Champaign*

***November 2011***

---

**TRANSPORTATION RESEARCH BOARD**  
OF THE NATIONAL ACADEMIES

## **INNOVATIONS DESERVING EXPLORATORY ANALYSIS (IDEA) PROGRAMS MANAGED BY THE TRANSPORTATION RESEARCH BOARD (TRB)**

This NCHRP-IDEA investigation was completed as part of the National Cooperative Highway Research Program (NCHRP). The NCHRP-IDEA program is one of the four IDEA programs managed by the Transportation Research Board (TRB) to foster innovations in highway and intermodal surface transportation systems. The other three IDEA program areas are Transit-IDEA, which focuses on products and results for transit practice, in support of the Transit Cooperative Research Program (TCRP), Safety-IDEA, which focuses on motor carrier safety practice, in support of the Federal Motor Carrier Safety Administration and Federal Railroad Administration, and High Speed Rail-IDEA (HSR), which focuses on products and results for high speed rail practice, in support of the Federal Railroad Administration. The four IDEA program areas are integrated to promote the development and testing of nontraditional and innovative concepts, methods, and technologies for surface transportation systems.

For information on the IDEA Program contact IDEA Program, Transportation Research Board, 500 5<sup>th</sup> Street, N.W., Washington, D.C. 20001 (phone: 202/334-1461, fax: 202/334-2081, <http://www.nationalacademies.org/trb/idea>)

The project that is the subject of this contractor-authored report was a part of the Innovations Deserving Exploratory Analysis (IDEA) Programs, which are managed by the Transportation Research Board (TRB) with the approval of the Governing Board of the National Research Council. The members of the oversight committee that monitored the project and reviewed the report were chosen for their special competencies and with regard for appropriate balance. The views expressed in this report are those of the contractor who conducted the investigation documented in this report and do not necessarily reflect those of the Transportation Research Board, the National Research Council, or the sponsors of the IDEA Programs. This document has not been edited by TRB.

The Transportation Research Board of the National Academies, the National Research Council, and the organizations that sponsor the IDEA Programs do not endorse products or manufacturers. Trade or manufacturers' names appear herein solely because they are considered essential to the object of the investigation.

## **NCHRP IDEA PROGRAM COMMITTEE**

### **CHAIR**

SANDRA Q. LARSON  
*IOWA DOT*

### **MEMBERS**

GARY A. FREDERICK  
*New York State DOT*  
GEORGENE GEARY  
*Georgia DOT*  
JOE MAHONEY  
*University of Washington*  
MICHAEL MILES  
*California DOT*  
JAMES M. SIME  
*Connecticut DOT*  
TOMMY E. NANTUNG  
*Indiana DOT*  
VALERIE SHUMAN  
*Shuman Consulting Group LLC*  
L. DAVID SUITS  
*North American Geosynthetics Society*

### **IDEA PROGRAMS STAFF**

STEPHEN R. GODWIN  
*Director for Studies and Special Programs*  
JON M. WILLIAMS  
*Program Director, IDEA and Synthesis Studies*  
INAM JAWED  
*Senior Program Officer*  
DEMISHA WILLIAMS  
*Senior Program Assistant*

### **EXPERT REVIEW PANEL**

MICHAEL SPRINKEL, *Virginia Transp. Research Council*  
VICKI PRILL, *Illinois Dept. of Transportation*  
ALEX APEAGYEI, *Virginia Transp. Research Council*  
PHIL BLANKENSHIP, *Asphalt Institute*  
JAMES BARNATT, *Road Science, LLC*  
TOM BROVOLD, *Test Quip, Inc.*

### **FHWA LIAISON**

DAVID KUEHN  
*Federal Highway Administration*

### **TRB LIAISON**

RICHARD CUNARD  
*Transportation Research Board*

### **COOPERATIVE RESEARCH PROGRAM STAFF**

CRAWFORD F. JENCKS  
*Deputy Director, Cooperative Research Programs*

**AN ACOUSTIC EMISSION-BASED TEST TO DETERMINE ASPHALT BINDER  
AND MIXTURE EMBRITTLEMENT TEMPERATURE**

**NCHRP IDEA Project 144**

**FINAL REPORT**

*Prepared by:*

William G. Buttlar

Behzad Behnia

Henrique M. Reis

University of Illinois at Urbana-Champaign

*Prepared for:*

**NCHRP IDEA PROGRAM  
TRANSPORTATION RESEARCH BOARD  
NATIONAL ACADEMIES**

November 2011

## TABLE OF CONTENTS

1. INTRODUCTION .....	6
2. ACOUSTIC EMISSION TESTING OF ASPHALT BINDERS .....	10
2.1. Experimental Procedure .....	11
2.1.1. <i>Materials Used</i> .....	11
2.1.2. <i>AE Sample Preparation</i> .....	13
2.1.3. <i>Acoustic Emission Testing Setup</i> .....	15
2.2. Analysis of Acoustic Emission Results .....	16
2.3. Results and Discussion .....	19
3. ACOUSTIC EMISSION TESTING OF ASPHALT MIXTURES .....	22
3.1. AE Testing of Loose Asphalt Mixtures .....	23
3.2. AE Testing of Compacted Asphalt Mixtures .....	25
3.2.1 <i>LTC Study Lab Compacted Asphalt Mixtures</i> .....	26
3.2.2 <i>Asphalt Institute Compacted Asphalt Mixtures</i> .....	28
3.2.3 <i>Mixtures Containing Recycled Asphalt Pavement (RAP)</i> .....	31
4. IMPROVED COOLING DEVICE .....	33
4.1. Thermoelectric Cooling System (TEC) .....	33
4.1. Shuttle ULT-25 Portable Freezer .....	37
REFERENCES .....	44
LIST of PUBLICATIONS .....	47

## List of Figures:

Figure 1. Typical Thermal Cracking in Asphalt Pavement.....	6
Figure 2. Nucleation, Propagation and Detection of AE Waves.....	8
Figure 3. Typical Acoustic Emission Signal.....	9
Figure 4. Schematic Representation of a Typical Acoustic Emission Testing Setup .....	9
Figure 5. (a) Rolling Thin Film Oven Test Setup for Short-Term Aging. (b) Pressure Aging Vessel Setup for Long-Term Aging. ....	12
Figure 6. Antioxidant Materials Utilized to Modify Asphalt Binders[9].....	13
Figure 7. Schematic Representation of AE Testing of Asphalt Binders.....	13
Figure 8. AE Sample Preparation Procedure. ....	14
Figure 9. (a) Top: Molds for Fabricating AE Samples; Bottom: Completed AE Sample in the Molds; (b) Typical Crack Patterns in Asphalt Binder Sample after AE Testing [2]. ....	15
Figure 10. AE Testing Setup [1] .....	15
Figure 11. Cooling Chamber with Dry Ice, Where a Thick Steel Plate Acts As a Heat Sink [2].....	16
Figure 12. Typical Temperature vs Time Cooling Plot .....	16
Figure 13. Typical Waveform Associated with an AE Event.....	17
Figure 14. Typical AE event Count Versus Temperature Plot Regions [18].....	18
Figure 15. Typical Plot of Event Count and AE Energy Versus Temperature .....	18
Figure 16. Mastic/Binder Coated Aggregate with Mounted AE Sensor.....	23
Figure 17. Binder Coated Aggregates.....	23
Figure 18. (a) AE Testing Set-up (b) AE Testing Specimen [11].....	25
Figure 19. Typical Plot of Event Count and AE Energy Versus Temperature .....	26
Figure 20. Thermally Induced Stresses within the Asphalt Mastic[18].....	26
Figure 21. Coring Site Locations: New Mexico, Montana [19]. ....	30
Figure 22. Sample Cores from Rounup, MT and Conchas Lake, NM[19].....	30

Figure 23. Embrittlement Temperature of RAP Mixtures Determined Using AE[20] .....	32
Figure 24. A Typical Thermoelectric Cooling Unit.....	33
Figure 25. Usage of Combination of P- and N-type Semiconductors in Thermoelectric Coolers.....	34
Figure 26. 4-Stage Peltier TEC Device with Cooling Chamber .....	34
Figure 27. TEC System Main Components: (a) 4-Stage Peltier TEC, (b) Cooling Chamber, (c) Temperature Controller (d) Power Supply.....	35
Figure 28. TEC system Wiring Diagram .....	36
Figure 29. TEC Device : (a) AE Asphalt Binder Test (b) AE Mixture Test.....	36
Figure 30. (a) Shuttle ULT-25 portable Freezer (b) Inside of ULT-25: The Cooling Chamber.....	38
Figure 31. The Free-piston Stirling Engine .....	38
Figure 32. Comparison between Free-piston Stirling Engine vs Conventional Refrigeration systems .....	39
Figure 33. Shuttle Portable Freezer Set Temperature Profile .....	39
Figure 34. Typical Linear Thermal Gradient of AE Sample for Average Applied Cooling Rate of 1°C/min .....	40
Figure 35. Different Applied and Measured Cooling Rates for Portable Freezer and AE Sample.....	40

## List of Tables:

Table 1. AE-based & BBR-based Cracking Temperatures of AOX-modified PG64-22.....	20
Table 2. AE-based & BBR-based Cracking Temperatures of AOX-modified PG70-22.....	20
Table 3. AE-based & BBR-based Cracking Temperatures of SHRP core Asphalt Binders.....	21
Table 4. AE-based & BBR-based Cracking Temperatures of SHRP core Asphalt Binders.....	22
Table 5. Binder, Binder Coated Aggregate, and Mastic Coated Aggregate Test Results.....	24
Table 6. Acoustic Emissions Test Results (Embrittlement Temperature and Temperature at Maximum Energy Event) .....	27
Table 7. Acoustic Emissions Test Results of Lab Compacted Mixtures .....	29
Table 8. Acoustic Emissions Test Results of Asphalt Institute Field Cores .....	31
Table 9. AE Test Results of TANK PG64-22 at Different Cooling Rates.....	41
Table 10. AE Test Results of TANK AAG1(PG58-16) at Different Cooling Rates .....	42
Table 11. AE Test Results of RTFO AAG1(PG58-16) at Different Cooling Rates .....	42



## **ACKNOWLEDGMENTS**

The authors gratefully acknowledge the support of all those who contributed to the success of NCHRP IDEA project#144, “An Acoustic Emission Based Test to Determine Asphalt Binder and Mixture Embrittlement Temperature”. The authors are thankful for the support provided by the NCHRP-IDEA program manager, Dr. Inam Jawed, and the IDEA project advisor, Dr. Michael Sprinkel of the Virginia Transportation Research Council. We would also like to thank the technical review panel members for their valuable inputs during the course of the study, which included Vicki Prill, Alex Apeagyei, Phil Blankenship, James Barnatt, and Tom Brovold. We would also like to thank Professor Mihai Marasteanu and Professor Zhanping You for providing binder samples, and the Asphalt Institute for providing mixture samples during the course of this study. Any opinions, findings, and conclusions or recommendations expressed in this publication are those of the authors and do not necessarily reflect the views of the sponsoring agency.

## 1. INTRODUCTION

A major form of deterioration in asphalt pavements constructed in cold climates is low temperature (or thermal) cracking, resulting from the restrained contraction of the asphalt mixture during cooling cycles. Pavement temperature is lowest at the surface and temperature changes are also the highest at the surface. Contractive strains induced by pavement cooling cause thermal tensile stress development in the restrained pavement layer. The induced thermal stresses are greatest in the longitudinal direction of the pavement (in the direction of traffic). Thermal cracking in the pavement manifests itself as transversely-oriented, surface-initiated cracks of various lengths and widths. For very severe cooling cycles (very low temperatures and/or very fast cooling rates) transverse thermal cracks may develop at specific locations within the pavement under one or very few cooling cycles. This is generally referred to as low-temperature cracking or single-event thermal cracking. Additional cracks will develop at different locations as the pavement is exposed to subsequent cooling cycles. For milder cooling conditions, cracks may advance and develop at a slower rate, such that it may take several cooling cycles for cracks to propagate completely through the surface layer. This is generally referred to as thermal fatigue cracking. Both phenomena are typically classified under the general category of thermal cracking in pavement engineering [1, 2, and 3].

A typical thermal cracking pattern occurring in asphalt pavements is shown in Figure.1. This form of distress drastically affects asphalt pavement life span, smoothness, and is associated with billions of dollars of repair and maintenance annually in the United States. If left untreated, thermal cracks will continue to deteriorate and widen over time, allowing moisture to readily infiltrate the pavement system. Detrimental effects of low-temperature cracking have motivated a number of studies in an effort to experimentally design and control asphalt properties related to the low temperature performance of asphalt pavements. However, accurate predictions of thermal cracking and associated failure mechanisms still remain a challenge [1].



**Figure 1. Typical Thermal Cracking in Asphalt Pavement**

As asphalt binder or mixture is cooled, it transitions from a brittle-ductile to a quasi-brittle physical state. In the quasi-brittle state, resistance to fracture is generally very low, allowing cracks to propagate readily. As a further complication, asphalt concrete tends to become oxidized, leading to material embrittlement with time. The amount of aging, or the aging rate, has been found to vary significantly depending upon crude source, refining techniques, additives, climate, and characteristics of the mixture (asphalt content,

air voids). As a consequence, one of the great challenges for the pavement engineer is to determine when a pavement surface has become vulnerable to embrittlement for a given climate [1].

Currently, the pavement engineer lacks practical tools to determine the proper time for preventive maintenance, such as the application of a surface treatment, or to determine when a more substantial rehabilitation is required, such as pavement milling and resurfacing. Another challenge facing the pavement engineer is the proliferation of new materials and the lack of field data to assess their suitability for a given climate. Such examples are: (1) recycled asphalt pavement (RAP) mixtures, particularly high RAP content mixtures, which are rapidly gaining popularity; (2) warm-mixes of which several varieties exist, having markedly different modification approaches; (3) open-graded mixtures; (4) stone mastic asphalt mixtures; (5) polymer-modified and acid-modified mixtures, where again, numerous polymers and modifiers exist, which impart substantially different physical properties to the mixture, and; (6) liquid antistripping agents. Combinations of these mixture types and/or modifiers are being used in the field, often without existing field performance to guide the designer in the material selection and mix design process. This can be problematic, since the result of blending acid modified mixtures with liquid anti-strip, for instance, is not well understood and can therefore lead to unexpected physical property changes.

In the case of RAP mixtures, the degree of blending between the new (virgin) and existing aged binder is difficult to determine, and moreover, the effect of this partial blending on the ability of the mixture to withstand cracking under low temperatures is difficult to assess. Warm mix additives are typically proprietary products, and range from zeolite-based additives, to organic additives, to low molecular weight esterified waxes. In addition, since these mixtures are produced at markedly lower production temperatures than conventional hot-mix, a practical tool is needed to assess their resistance to low temperatures in the as-built condition.

The NCHRP-IDEA Project 144 focused on the development of a simple and practical Acoustic Emission-based testing method for the accurate and rapid characterization of the cracking behavior of asphalt binders and mixtures. In addition to asphalt binders and hot mix asphalt, this technique can be implemented to characterize modern warm mix asphalt and mixtures with high amounts of RAP, to help ensure the durability of these environmentally friendly materials. This research project consisted of two phases. Work in phase 1 focused on the standardization and validation of method for binder testing along with the development of an improved prototype of an asphalt embrittlement device. In phase 2, techniques for using the AE-based device for the characterization of asphalt mixtures were developed. In phase two, two mixture specimen configurations were investigated: (1) loose mixture (aggregates coated with asphalt); (2) compacted asphalt mixture (compacted with the Superpave gyratory compactor or specimens fabricated from field-compacted samples). A comprehensive research effort was undertaken to accomplish the proposed tasks. In this report, the Acoustic Emission technique is first introduced, followed by documentation outlining the development of AE testing methods for asphalt binders and asphalt mixtures. Extensive lab sample test results and field validation data are presented, along with recommendations for implementation and future study.

The Acoustic Emission (AE) testing technique is a recognized nondestructive testing (NDT) method. It is defined as the spontaneous release of localized strain energy in a stressed material which can be recorded using sensitive acoustical sensors. The terms “Acoustic Emission” and “Acoustic Emission signal” are often used interchangeably. Strictly speaking, an acoustic emission is a mechanical elastic wave generated by a material and an AE signal is the electrical signal produced by a sensor in response to this wave. The characteristics of the signal derive from the mechanism that generated the emissions, the path by which the waves travel through the material, and finally, the sensor which transforms the emission into a signal [4, 5, and 6].

AE testing is a very commonly employed technique to detect and locate faults in mechanically loaded structures and components. The AE technique has proven itself to be a powerful tool for examining the behavior of materials deforming under stress and has been extensively applied for condition assessment and damage detection for many materials such as steel, concrete, wood, etc. Almost all materials produce acoustic emissions when they are stressed beyond their normal design ranges to final failure [4, 5, and 6].

Familiar examples of AE events are the creaking of timber subjected to loading near failure or the cracking sound generated when stepping onto a thin layer of ice; the sounds from timber or ice layer are used as indicators of the impending failure of material's structure. Acoustic Emission in this form is to the ears what visual inspection is to the eyes [4]. The analysis of these emissions has become a science in itself. AE is currently experiencing an increase in popularity due to advances in high-speed digital waveform-based AE instrumentation which allows vast numbers of AE waveform signals to be digitized and stored for analysis. Moreover, high sensitivity broadband sensors and development of advanced signal analysis software have played an important role in the increased usage of the AE technique [4].

AE testing is based on the fact that solid materials emit sonic or ultrasonic acoustic emissions when they are mechanically or thermally stressed to the point where damage or fracturing occurs. During plastic deformation, dislocations and micro-cracks move through the material's structure producing AE stress waves, which can be most optimally obtained over short distances and under controlled conditions, such as in the laboratory [5, 6].

The AE test method detects, locates, identifies, and produces other data describing the physical nature of flaws as they are generated in a stressed object. The method provides comprehensive information on the origin of a flaw in a stressed component and can also provide information pertaining to the development of this flaw as the component is subjected to stress. For instance, it is a very sensitive indicator of crack propagation [4]. AE waves from a growing flaw travel within the material and are detected by sensitive surface-mounted sensors. Figures 2 and 3 schematically illustrate crack nucleation and propagation and corresponding AE wave transmission and detection for a material under stress and the typical AE signal, respectively.

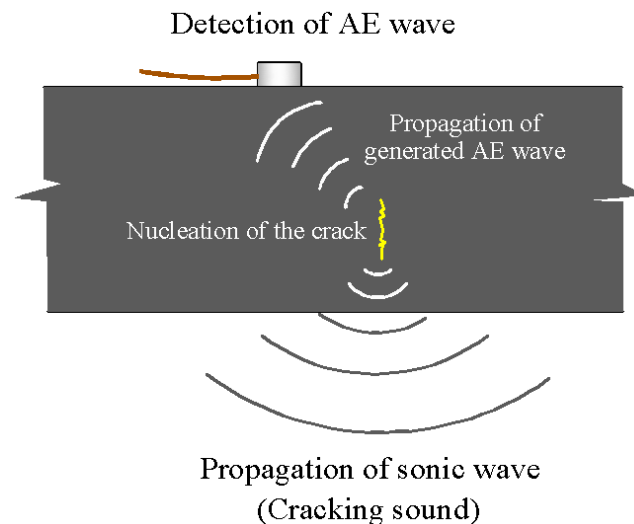


**Figure 2. Nucleation, Propagation and Detection of AE Waves**

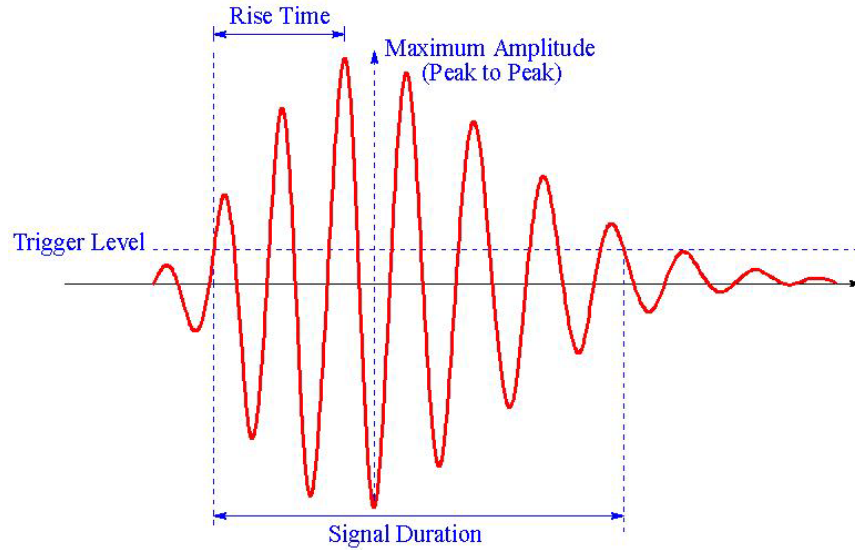


**Figure 3. Typical Acoustic Emission Signal**

One of the advantages compared to other NDE techniques is the possibility to observe the time-dependent damage process during the entire load history. To do so, the application of signal-based methods requires reliable localization, i.e. the determination of the source coordinates of the events [4, 5].

Acoustic emission stress waves can be measured using piezoelectric transducers. Problems arise in the low level magnitude of the emission activity and the high frequency of the signal. The microfracturing processes leading to failure of a material are generally short-lived events with rise times on the order of  $10^{-6}$  to  $10^{-4}$  seconds. Emissions or stress waves generated by these processes are low level in magnitude; therefore, special electronic equipment is required for detection, recording, and analysis. Figure 4 schematically represents a typical AE testing setup. AE stress waves are detected with an electromechanical transducer, amplified, filtered, and then recorded. A well-conceived test procedure, good equipment, and adequately skilled personnel are prerequisites for successful AE testing. The test procedure must take into account probable sources of emission, possible background noise, and load history of the material [4, 5, and 6].

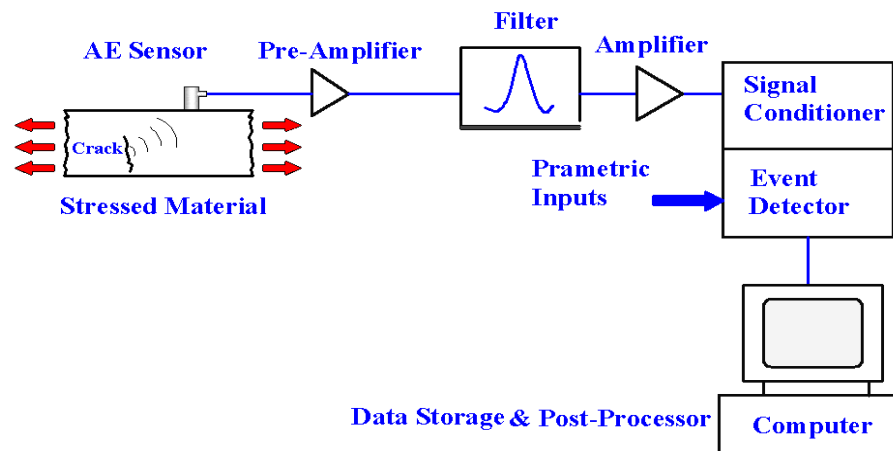


**Figure 4. Schematic Representation of a Typical Acoustic Emission Testing Setup**

## 2. ACOUSTIC EMISSION TESTING OF ASPHALT BINDERS

Properties of the asphalt binder are generally believed to be among the most important factors related to low temperature cracking of asphalt pavements [7]. For a given pavement, the cracking temperature of its asphalt binder is considered to be a good indicator of the low-temperature cracking resistance of the pavement [2].

Various test parameters and temperature susceptibility-based criteria have been proposed in the past to help control thermal cracking of asphalt pavements. These include: penetration at 25°C, kinematic viscosity at 135°C, McLeod's dimensionless Pen-Vis Number (PVN) and Penetration Index (PI) [7]. McLeod's dimensionless Pen-Vis Number (PVN) is defined by the following relation [7]:

$$PVN = \frac{-1.5(L - \log_{10} \eta)}{(L - M)}$$

Where:

$$L = 4.25800 - 0.79674 \log_{10}(PEN)$$

$$M = 3.46289 - 0.61094 \log_{10}(PEN)$$

$\eta$  = Kinematic viscosity at 135°C (cSt)

PEN = Penetration at 25°C (dmm)

Susceptibility criteria of the asphalt binder have been defined as follows:

$$\begin{aligned} PVN > -0.6 & \text{ low thermal susceptibility} \\ -1.0 < PVN < -0.6 & \text{ moderate thermal susceptibility} \\ PVN < -1.0 & \text{ high thermal susceptibility} \end{aligned}$$

Penetration Index (PI) is defined by the following relationship:

$$PI = \frac{20 - 500B}{50B + 1}$$

Where

$$B = \frac{\log_{10}(PEN(T_1)) - \log_{10}(PEN(T_2))}{T_1 - T_2}$$

B represents the slope of the log penetration versus temperature relationship. Asphalt binders with PI values below -1.5 are considered to be susceptible to thermal cracking [7].

In the early 1990's, Superpave binder tests developed under the Strategic Highway Research Program (SHRP) improved the manner in which asphalt binders are specified and purchased (AASHTO MP1). This was accomplished by implementing fundamental material tests over a broad range of production and service temperatures. However, these tests were not developed for highly modified binders, and were not developed for the design and control of RAP and warm-mix materials. Although the BBR has correlated well to thermal cracking in the field for straight run binders, it is more appropriate to employ the direct tension test (DTT) in conjunction with the BBR as an option in the AASHTO M320 specification to enable a broader range of binders to be evaluated. However, the DTT device suffers from poor repeatability, is relatively expensive, and requires significant operator training and care. In addition, the combination of the BBR and DTT carries an equipment cost in the range of \$70 - \$80k. Very few agencies currently have access to the DTT test, and the future of the DTT as a standardized test method is uncertain.

For the practical low-temperature evaluation of binders, binder blends, and mixtures for the purpose of formulation, design, control, and forensics, there is still a need for a test which is: rapid; simple; compact and portable; applicable to modern materials (highly modified, recycled, warm-mix); versatile, able to test binders and mixtures and suitable for lab-produced and field materials; extendable to in-situ pavement evaluation; capable of testing thin mixture specimens, independent of size effect, and; designed specifically to aid in the timing and selection of preventive maintenance and rehabilitation treatments [2]. The Acoustic Emission-based testing technique developed in this study addresses the current shortage of accurate, practical, field-ready tests for low-temperature characterization of asphalt binder and mixtures. The use of AE testing for evaluating bituminous materials dates back several decades. Khosla and Goetz [8] used AE techniques to detect crack initiation and propagation in indirect tensile (IDT) specimens at -23°C. The study found that failure by fracture is indicated by a sharp increase in total AE counts and that significant AE counts occur at about 80% of the peak load. Valkering and Jongeneel [9] used the AE technique to monitor temperature cycling tests with restrained asphalt concrete specimens at low temperatures (10°C to -40°C). They observed that the repeatability of AE measurements is good, that the AE activity (number of events) correlates with thermal fracture temperatures, and that the AE activity in restrained specimens at low temperatures is caused by defect initiation in the binder. Hesp, et al. [10] used AE measurements to detect crack initiation and propagation in restrained specimens at low temperatures (-32° to -20°C). They concluded that the SBS-modified mixes produced less AE activity than unmodified mixes. Li et al. [11] used AE techniques to characterize fracture in semi-circular bend asphalt specimens at low temperatures (-20 °C). They concluded that large amounts of accumulated AE events occur at 70% of material strength, that the maximum intensity of AE peaks correlates with the development of macrocracks, and that the location of AE events suggests that a several centimeter-sized process zone forms before peak load. Nesvijski and Marasteanu [12] used an AE spectral analysis approach to characterize fracture in semi-circular bend asphalt specimens at low temperatures, and concluded that an AE approach could be used for evaluation of asphalt pavements [2]. It should be noted that all of the previous studies involved the need for mechanical mixture tests, which are relatively expensive and time-consuming to perform as compared to the techniques proposed herein. The first phase of the NCHRP IDEA project#144 was focused on the development of a rapid and practical AE-based technique to characterize the low temperature cracking behavior of asphalt binders. Rheological properties of the binders obtained using the BBR device was used to determine BBR-based critical cracking temperatures. Obtained AE-based cracking temperatures were then compared to BBR-based results. Other tests and observations made by testing a wide range of binders for the purpose of test evaluation and optimization are also presented in the sections that follow [1, 2, and 13].

## **2.1. Experimental Procedure**

### ***2.1.1. Material Used***

The AE testing technique was employed to determine the “Embrittlement” temperature of a wide range of asphalt binders. Several different types of asphalt binders, which were processed to different aging levels, were tested as follows:

- Anti-oxidant (AOX) Modified Asphalt Binders:

PG64-22, PG70-22, AOX-modified PG64-22, AOX-modified PG70-22

- Asphalt Binders from an ongoing pooled fund study (#776) on low-temperature cracking:

PG64-22 (NY), PG58-28 (MN/Road-section20), PG58-34 (MN/Road- section22)

- Strategic Highway Research Program (SHRP) core asphalt binders:

AAG-1 (PG 58-16), AAD-1(PG58-28), AAA-1(PG58-28), and AAF-1(PG64-22))

- Sasobit-modified Warm Mix Asphalt Binder (PG64-22)

All binders were aged using the Rolling Thin Film Oven (RTFO) according to ASTM D2872–04 and the Pressure Aging Vessel (PAV) in accordance with ASTM D6521–05. The RTFO Test is a short-term sample conditioning procedure for asphalt binders that simulates the aging that takes during hot-mix production, plus about two years of in-field aging. During the RTFO Test, a 35 g asphalt sample in the form of a 1.25 mm thin film of asphalt is exposed to both heat (163 °C) and air flowing at a rate 400ml/min for 85 minutes in an oven with a rotating rack revolving at speed of 15 rpm. The PAV Test simulates the long term aging of the binder after about 10 years of service. During PAV testing, a 50 g sample of RTFO-aged sample is subjected to 2.1 MPa air pressure at a temperature of 100 °C for 20 hours. Figure 5 shows the RTFO and PAV test equipment used in this study [14, 15, and 16].



**Figure 5. (a) Rolling Thin Film Oven Test Setup for Short-Term Aging. (b) Pressure Aging Vessel Setup for Long-Term Aging[15]**

To prepare AOX-modified binders, two asphalt binders, namely PG 64-22 and PG 70-22 were selected, primarily because they exhibit very different aging and thermal cracking susceptibility characteristics. In addition, half of the asphalt binder samples were modified using an antioxidant (AOX) treatment prior to conditioning and testing. Among several different antioxidant materials, a combination of two additives, namely: Dilaurylthiodipropionate (DLTDP) and Furfural together with hydrochloric acid as catalyst was utilized in this study. Apeagyei et al. [8] showed that this combination provided the best resistance to oxidative aging in laboratory-aged asphalt binders. AOX-modified asphalt binders were prepared by mixing antioxidants in the following order: Hydrochloric acid (1.2%), Furfural (2%), and DLTDP (1.5%), as illustrated in Figure 6. A Barnant mixer operating at a speed of 750 rpm was used to incorporate the antioxidants into the base asphalt. The total mixing time was 4 hours; DLTDP was introduced after the second hour in three divided portions. The mixing temperature was kept constant at about 115 °C. During this period the mixture was continuously stirred with the Barnant Mixer. Un-aged (tank) samples of all the binders were tested. In addition, both unmodified and AOX-modified asphalt binders were short-term



aged using the Rolling Thin Film Oven (RTFO) in accordance to standard ASTM D2872–04 also long-term aged in a pressure aging vessel (PAV) in accordance with ASTM D6521–05 [14,15,16].

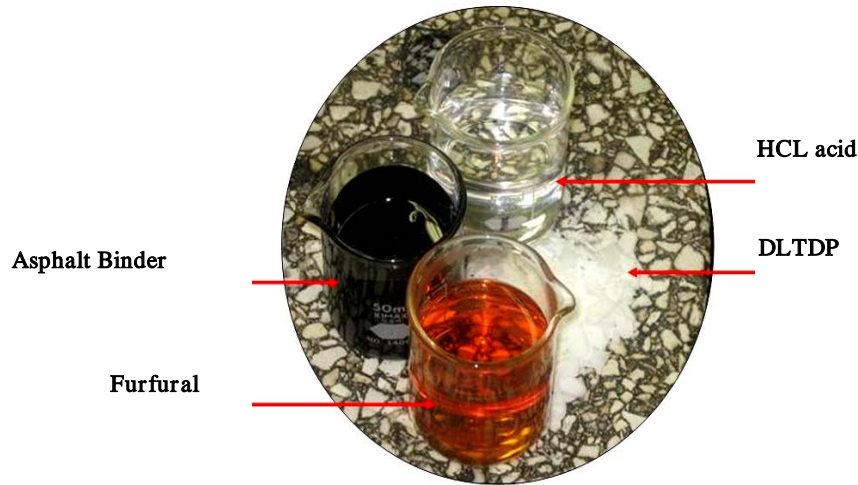


**Figure 6. Antioxidant Materials Utilized to Modify Asphalt Binders[9]**

### **2.1.2. AE Sample Preparation**

In order to evaluate the low temperature cracking performance of asphalt binders, thin films of asphalt binders were bonded to granite substrates and exposed to decreasing temperatures, ranging from 20 °C to -50 °C. Differential thermal contraction between granite substrates and asphalt binders induces progressively higher thermal stresses in the binders resulting in thermal crack formation, which is accompanied by a release of elastic energy in the form of transient waves. The critical cracking temperatures of the asphalt binders tested were predicted by processing and analyzing the emitted elastic waves captured during the tests using the AE technique. Figure 7 schematically illustrates an AE testing sample of asphalt binder with a granite substrate. [1, 2].

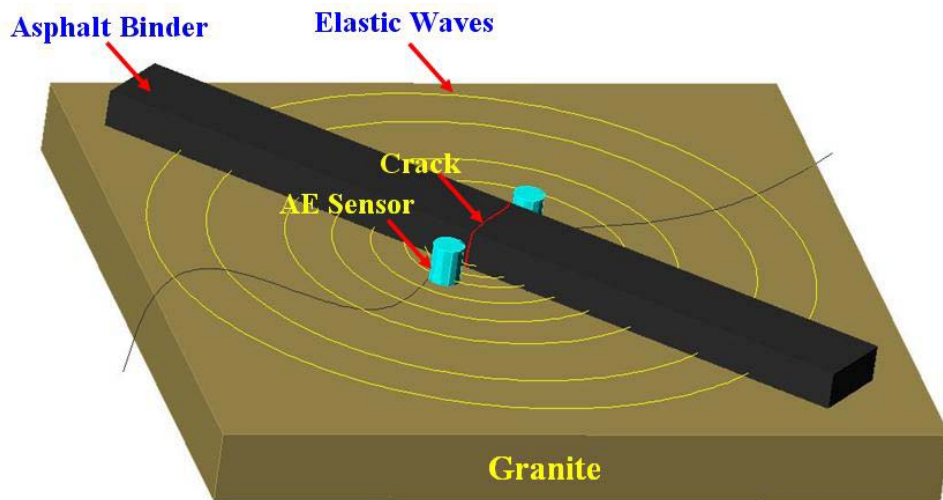


**Figure 7. Schematic Representation of AE Testing of Asphalt Binders**

The thin, rectangular asphalt binder samples used in the AE test were generally molded to be identical to standard BBR sample dimensions. Teflon tape was used as a debonding aid during molding, as shown in Figures 8 and 9. A 10 mm thick square granite slab (150 mm by 150 mm) was used as the substrate. In order to ensure proper bonding and restraint between the asphalt binder sample and the substrate, the granite substrate was preheated to about 120°C. The mold was placed on the heated slab and asphalt binder at a temperature of 135°C was poured into the mold. The AE sample preparation procedure is shown in Figure 8. At the end of each test, bonding was verified by the absence of visual debonding, even after visible transverse cracks at regular spacing were present (Figure 9). It was observed that the sample preparation procedure guaranteed a very good bond in each of the binder samples tested [1].



**Figure 8. AE Sample Preparation Procedure**



**Figure 9. (a) Top: Molds for Fabricating AE Samples; Bottom: Completed AE Sample in the Molds; (b) Typical Crack Patterns in Asphalt Binder Sample after AE Testing [2]**

### ***2.1.3. Acoustic Emission Testing Setup***

Prepared AE samples are positioned on a steel block in the cooling chamber as shown in Figures 10 and 11. AE tests were conducted in a polystyrene box containing dry ice as the coolant. The temperature was recorded using a K-type thermocouple, which was placed adjacent to the asphalt sample at the interface between the substrate and asphalt binder specimen. Figure 12 shows a typical temperature versus time cooling profile. In order to be as consistent as possible, the amount of dry ice inside the polystyrene box is kept constant. Wideband AE sensors (Digital Wave, Model B1025) with a nominal frequency range of 50 kHz to 1.5 kHz were utilized to monitor and record acoustic activities of the sample during the test. High-vacuum grease was used to couple the AE sensors to the granite substrate. Signals from three AE sensors were pre-amplified 20dB using broad-band pre-amplifiers to reduce extraneous noise. The signals were then further amplified 21 dB (for a total of 41 dB) and filtered using a 20 kHz high-pass double-pole filter using the Fracture Wave Detector (FWD) signal condition unit. The signals were then digitized using a 16-bit analog-to digital converter (ICS 645B-8) using a sampling frequency of 2 MHz and a length of 2048 points per channel per acquisition trigger. The outputs were stored for later processing using Digital Wave software (WaveExplorer™ V7.2.6).

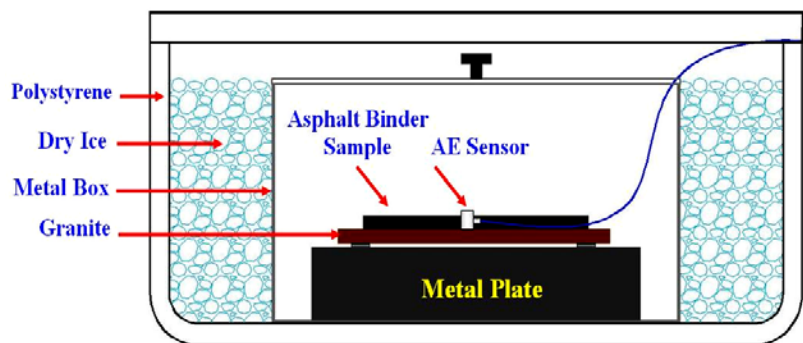


**Figure 10. AE Testing Setup [1]**



**Figure 11. Cooling Chamber with Dry Ice, where a Thick Steel Plate Acts as a Heat Sink [2]**

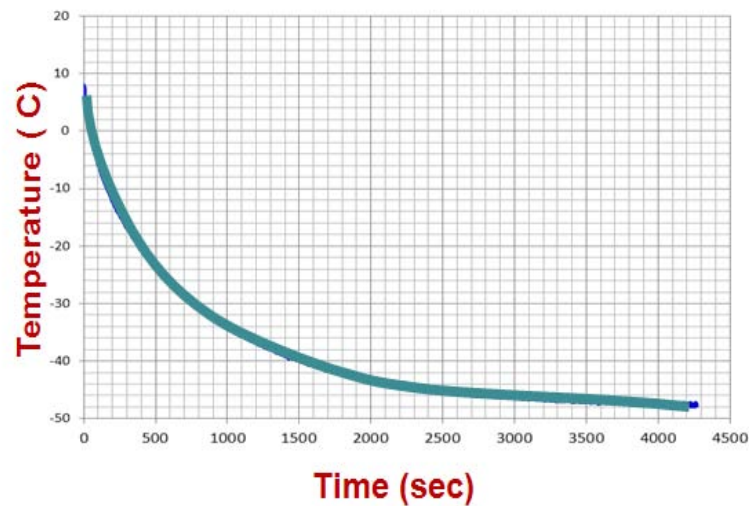


**Figure 12. Typical Temperature vs. Time Cooling Plot**

## 2.2. Analysis of Acoustic Emission Results

Evaluation of AE activity during thermal loading of asphalt binder samples is performed on recorded event signals and associated test temperature. A typical waveform associated with an AE event is shown in Figure 13. An AE event is hereafter referred to as a local material change giving rise to a measurable acoustic emission. It is an individual waveform having a threshold voltage of 0.1 V and energy equal to or greater than  $4 \text{ V}^2\text{-}\mu\text{s}$ . The emitted energy associated with each event is one of the characteristics of an AE signal and can be computed using the equation shown below, where  $E_{\text{AE}}$  is AE energy of an event ( $\text{V}^2\text{-}\mu\text{sec}$ ) with duration of time  $t$  ( $\mu\text{sec}$ ) and recorded voltage of  $V(t)$ .



$$E_{AE} = \int_0^t V^2(t)dt$$

“Noise” is a major issue in acoustic emission analysis, where noise is simply defined as any unwanted signal captured by the AE system. There is a need to separate genuine stress wave emissions, originating from within the material, from noises such as environmental noise, mechanical noise (movement of the component or sensor during testing), electrical noise, etc. An essential step in a properly conducted AE test is the elimination or filtering of noise, which can be accomplished through appropriate equipment design and testing techniques. Much of this can be achieved by careful electronic filtering of the received AE data, but best practice involves the identification and removal of as many sources of extraneous noise as possible prior to testing. In this study, to minimize the amount of extraneous data including electronic noise, the piezoelectric AE sensors were conditioned in the cooling chamber prior to starting of test. In addition, all events with energy lower than 100 V<sup>2</sup>-μs were filtered out. All results presented hereafter are based on the above filtering procedures.

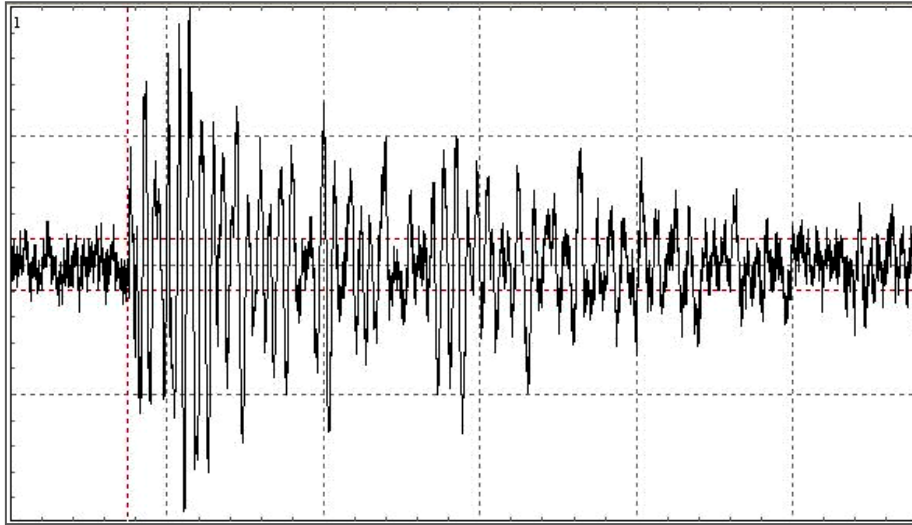


**Figure 13. Typical Waveform Associated with an AE Event**

A typical plot of event counts versus temperature for typical asphalt binder and mixture AE tests are shown in Figure 14. Three distinct regions were found to exist in AE event count versus temperature plots, namely: pre-cracking, transition and stable cracking regions. During the pre-cracking region, differential thermal contraction between the asphalt binder and the granite substrata cause thermal stresses to accumulate in the binder specimen eventually leading to material fracture. In the “Pre-cracking region,” no AE events are detected. Progressively higher thermal stresses in the specimen result in the formation of thermal microcracks in the material, which is accompanied by the release of elastic waves. This manifest itself as a cluster of high amplitude waves during the test. The transition region is defined as the point in time when thermal microcracking in the specimen, as indicted by higher energy events, begins to occur. The temperature corresponding to the event with the first peak energy level has been termed the “Embrittlement temperature,” as shown in Figure 15. It is hypothesized that the embrittlement temperature represents a fundamental material state which is independent of material constraint, sample size (as long as a statistically representative volume or larger is used), and sample shape [18].

The “transition region” can be considered as the region where material behavior gradually changes from a quasi-brittle to a brittle state and where resistance to fracture is generally very low, allowing cracks to propagate readily. The “stable cracking region” usually initiates at a very low temperature, when the material is brittle and generates a significant amount of AE activity. Based upon examination of the study data, this regime is thought to be below the glass transition region of the binder. The AE event count versus temperature plot in this region usually has a steep slope that remains relatively constant. The microcracking results primarily from a combination of asphalt binder or mastic brittleness and the action of tensile thermal stresses within the material.

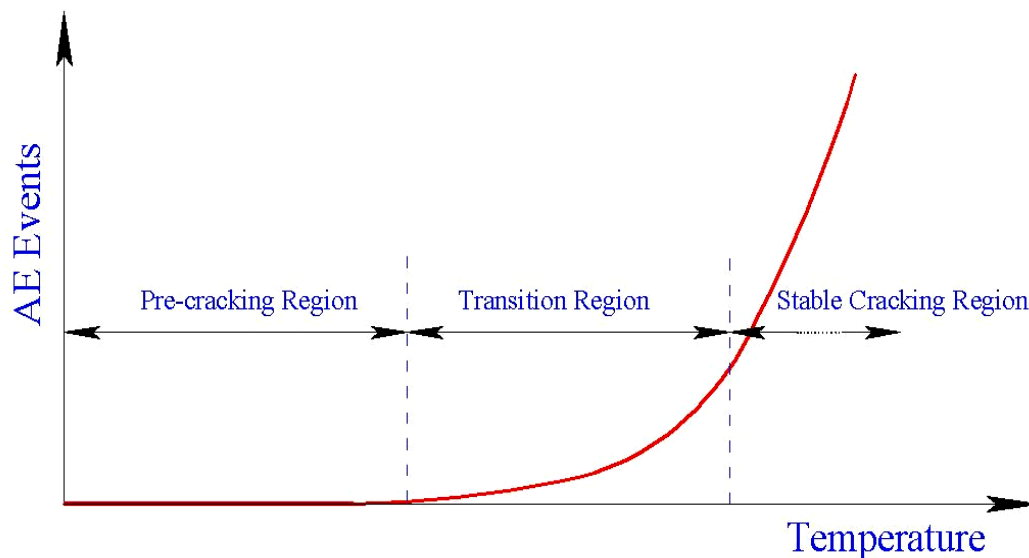


**Figure 14. Typical AE event Count Versus Temperature Plot Regions [18]**

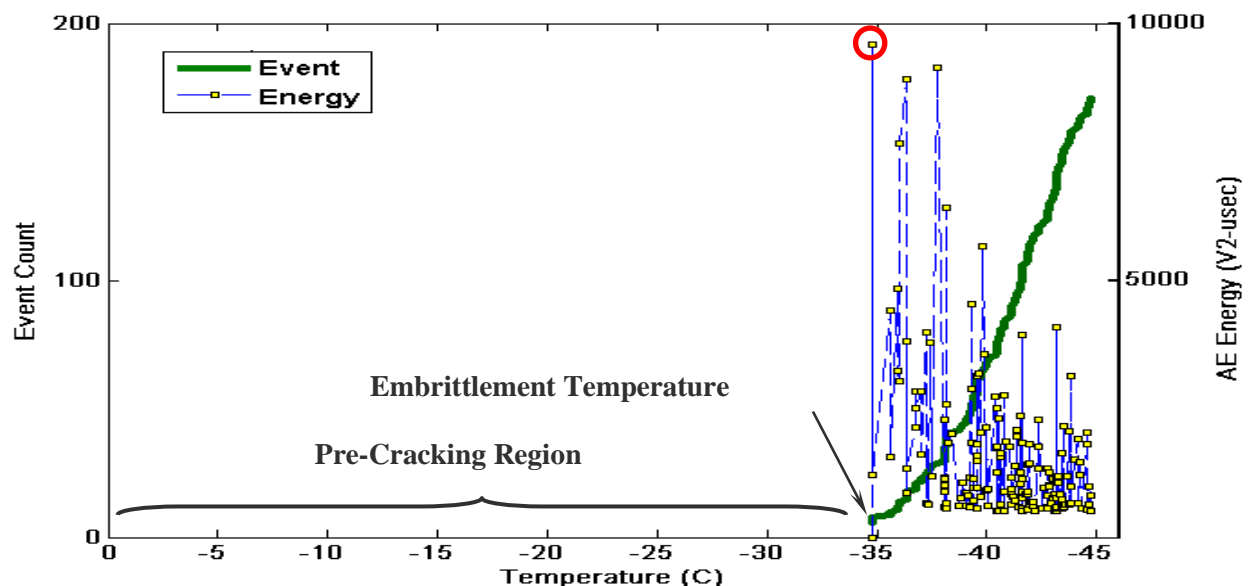


**Figure 15. Typical Plot of Event Count and AE Energy Versus Temperature**

### 2.3. Results and Discussion

The embrittlement temperature ( $T_{EMB}$ ) of asphalt binders evaluated through AE testing is now compared with the critical cracking temperature ( $T_{CR}$ ) obtained from the Superpave asphalt binder test procedures. The critical cracking temperature for the asphalt binders were determined using the test results described by Marasteanu et al. (LTC Phase-I Report) and using the procedure described in NCHRP Report 452. The equation used for determining critical temperature using Superpave tests is shown below for the case of creep stiffness (S value) from BBR test.

$$T_{CR} = T_1 + \left( \frac{\log(300) - \log(S_1)}{\log(S_2) - \log(S_1)} \right) (T_2 - T_1)$$

Where,  $S_1$  and  $S_2$  are BBR creep stiffnesses at test temperatures of  $T_1$  and  $T_2$ , respectively. When using direct tension test (DTT) results, a similar interpolation technique can be used to determine the temperature at which a failure strain of 1% is reached. Embrittlement temperatures along with thermal cracking temperatures for various asphalt binders tested at different age conditioning levels are provided in Tables 1 through 4. In all cases, a minimum of 3 replicates were used to produce the average values and statistical measures presented in this section. The coefficient of variation (COV) is computed by dividing the standard deviation of a population (in this case, embrittlement temperature or cracking temperature) by the absolute value of the sample mean. Strictly speaking, the COV statistic is most appropriate for data measured on a ratio scale, unlike temperature, which is expressed on an interval scale. Thus, the COV statistic will be temperature-scale dependent (different results would be obtained for results expressed in degrees Kelvin versus degrees Celsius, for instance), and would produce infinite values for means approaching zero. For the present application, where embrittlement temperatures were in a relatively narrow range and sufficiently below zero, the COV statistic was deemed to be a useful statistical parameter to describe the repeatability of the measurements obtained.

Tables 1 and 2 summarize measured embrittlement and cracking temperatures based on AE and BBR testing methods for AOX-modified PG64-22 and PG70-22. The results show that Embrittlement temperatures ( $T_{EMB}$ ) obtained from the AE method for AOX-modified binders are slightly lower than BBR-based cracking temperatures for unmodified binders. This is not unexpected, since the BBR stiffness threshold (upper limit of 300 MPa) was established with an inherent factor of safety to avoid low temperature cracking. The results also suggest that adding AOX to asphalt binder improves its low temperature performance by lowering its cracking temperature, which is consistent with the results obtained from BBR testing. Comparing AE and BBR results also reveals a very strong correlation between the two methods.

**Table 1. AE-based & BBR-based Cracking Temperatures of AOX-modified PG64-22**

Sample ID	AE-based Embrittlement Temperature		BBR-based Cracking Temperature (°C)
	T <sub>EMB</sub> (°C)	CoV (%)	
TANK-PG64-22	-29.5	6.2%	-28.6
TANK-PG64-22+AOX	-30.7	2.0%	-31.9
RTFO-PG64-22	-26.9	3.8%	-27.9
RTFO-PG64-22+AOX	-28.9	2.4%	-29.8
PAV-PG64-22	-23.3	6.3%	-24.2
PAV-PG64-22+AOX	-26.7	6.0%	-27.6

**Table 2. AE-based & BBR-based Cracking Temperatures of AOX-modified PG70-22**

Sample ID	AE-based Embrittlement Temperature		BBR-based Cracking Temperature (°C)
	T <sub>EMB</sub> (°C)	CoV (%)	
TANK-PG70-22	-24.8	6.3%	-25.8
TANK-PG70-22+AOX	-31.5	8.1%	-30.3
RTFO-PG70-22	-23.4	5.3%	-24.6
RTFO-PG70-22+AOX	-28.6	7.2%	-29.9
PAV-PG70-22	-22.5	6.7%	-23.8
PAV-PG70-22+AOX	-27.5	3.8%	-28.0



Embrittlement and cracking temperatures for SHRP core binders and LTC study binders are presented in Tables 3 and 4, respectively. These results indicate the expected outcome that the critical cracking temperature of an asphalt binder is sensitive to aging level, where  $T_{\text{cracking}}(\text{TANK}) < T_{\text{cracking}}(\text{RTFO}) < T_{\text{cracking}}(\text{PAV})$ . The COV levels for AE tests conducted on the SHRP and LTC study binders were lower than the COV values obtained when testing the AOX-modified binders. This can be attributed to preconditioning the AE sensors in the cooling chamber prior to testing of the SHRP and LTC study binders, whereas this technique had not yet been discovered at the time of AOX sample testing.

**Table 3. AE-based & BBR-based Cracking Temperatures of SHRP core Asphalt Binders**

Sample ID	AE-based Embrittlement Temperature		BBR-based Cracking Temperature (°C)
	$T_{\text{EMB}} (^\circ\text{C})$	CoV (%)	
TANK-AAA1	-36.3	1.7%	-34.5
RTFO-AAA1	-35.4	2.0%	-32.3
PAV-AAA1	-30.9	1.9%	-29.7
TANK-AAD1	-37.2	1.3%	-34.4
RTFO-AAD1	-35.9	1.9%	-33.1
PAV-AAD1	-30.6	1.5%	-30.1
TANK-AAF1	-24.6	1.8%	-25.4
RTFO-AAF1	-21.1	1.3%	-24.7
PAV-AAF1	-18.7	2.6%	-20.4
TANK-AAG1	-20.7	2.9%	-20.0
RTFO-AAG1	-19.2	2.1%	-19.1
PAV-AAG1	-17.2	1.5%	-17.0

**Table 4. AE-based & BBR-based Cracking Temperatures of SHRP Core Asphalt Binders**

Sample ID		AE-based Embrittlement Temperature		BBR-based Cracking Temperature (°C)
		T <sub>EMB</sub> ( °C )	CoV (%)	
<b>MnRoad20 (PG58-28)</b>	<b>Tank</b>	<b>-35.0</b>	<b>0.8%</b>	<b>-31.9</b>
	<b>RTFO</b>	<b>-34.5</b>	<b>4.2%</b>	<b>-30.0</b>
	<b>PAV</b>	<b>-30.2</b>	<b>2.1%</b>	<b>-28.3</b>
<b>MnRoad20 (PG58-34)</b>	<b>Tank</b>	<b>-43.4</b>	<b>3.2%</b>	<b>-36.9</b>
	<b>RTFO</b>	<b>-40.7</b>	<b>2.3%</b>	<b>-35.5</b>
	<b>PAV</b>	<b>-38.5</b>	<b>1.0%</b>	<b>-34.2</b>
<b>NY (PG64-22)</b>	<b>Tank</b>	<b>-30.3</b>	<b>3.0%</b>	<b>-27.4</b>
	<b>RTFO</b>	<b>-28.6</b>	<b>1.8%</b>	<b>-27.1</b>
	<b>PAV</b>	<b>-25.5</b>	<b>1.4%</b>	<b>-22.9</b>

### 3. ACOUSTIC EMISSION TESTING OF ASPHALT MIXTURES

Asphalt pavement is a heterogeneous material composed of the asphalt binder and aggregates. Upon rapid cooling, asphalt mastic in the pavement contracts more than aggregates particles causing thermal stresses in the pavement to develop. When temperatures drop below the point where asphalt mastic becomes brittle, thermal cracking can develop in the asphalt pavement. The AE testing technique was employed to explore this phenomenon, through mastic and mixture testing.

Currently, mechanical tests such as the Superpave Indirect Tension Test (IDT)[17], Disk-Shaped Compact Tension Test (DC[T]), Semi- Circular Bend Test (SCB), and Thermal Stress Restrained Specimen Test (TSRST) are available to assess thermal cracking potential of asphalt pavements. While these tools provide a closer link to field performance by testing the entire asphalt mixture, they are currently neither convenient nor cost effective for employment in practical mix design and evaluation. The cost of these devices are in the range of \$50k - \$150k depending upon test device features and require specimen sawing, and in some cases, coring and/or notch fabrication. It is also difficult to assess near-surface properties and severe aging gradients, which may be the key to the initiation and propagation of thermal and block cracks and possibly top-down fatigue cracks. The acoustic emission-based testing method offers a potentially simpler and less costly alternative to evaluate the low temperature crack resistance of asphalt-aggregate mixtures.

Given this background, the second phase of this project involved the implementation of the AE-based testing technique and standardization of testing methods for asphalt mixtures. Two specimen configurations were proposed:

- (1) Loose mixture (aggregates coated with asphalt binder)
- (2) Compacted asphalt mixture (compacted with the Superpave gyratory compactor, for instance)

Testing setup and data analysis are identical to asphalt binder AE test. In the following, AE asphalt mixture testing for both loose mixtures and compacted mixtures are explained in details along with obtained test results.

### 3.1. AE Testing of Loose Asphalt Mixtures

Different types of asphalt binders including PG 64-22, PG 70-22, PG58-28, and Sasobit-modified asphalt binder (a warm-mix asphalt additive) were utilized to prepare loose (uncompacted) asphalt mixtures. AE testing was conducted on individual aggregates coated with mastic. In addition to mastic coated aggregates, individual aggregates coated with asphalt binder were also examined. In both cases, as illustrated in Figure 16, the AE sensor was mounted on the mastic/binder coated aggregate and monitoring of the AE activity of the specimen was accomplished as specimen cooling occurred. Binder-coated- and mastic-coated-aggregates are shown in Figures 17(a) and 17(b), respectively.

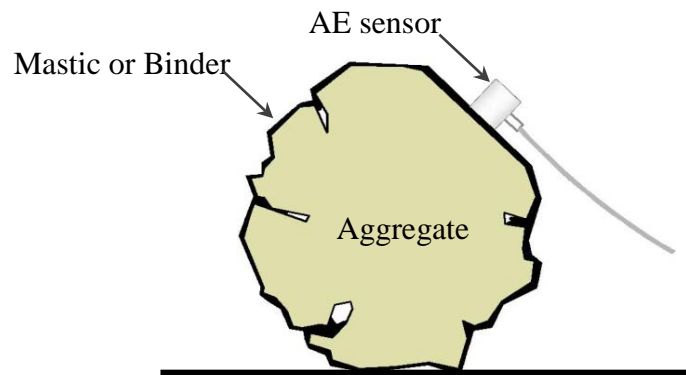


**Figure 16. Mastic/Binder Coated Aggregate with Mounted AE Sensor**

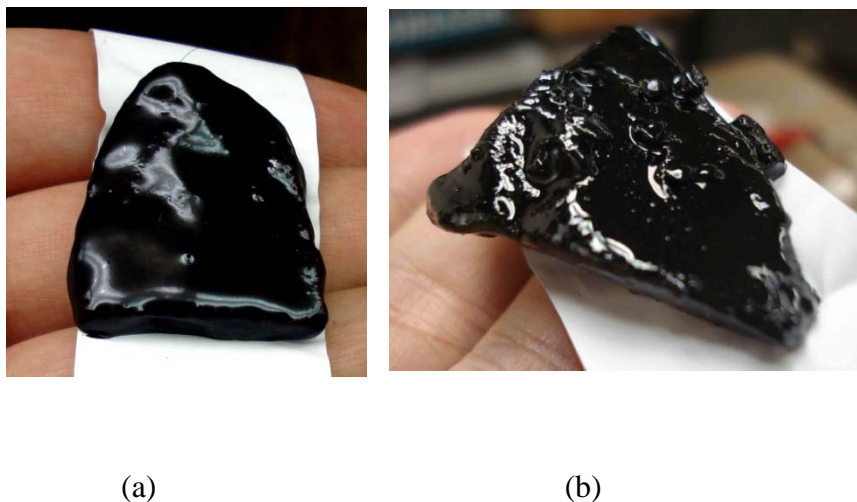


**Figure 17. Binder Coated Aggregates**

Table 5 summarizes the results obtained from testing of binder and mastic coated aggregate particles. It was observed that the embrittlement temperature of mastic coated aggregates was slightly lower than that of binder coated aggregates. However, comparing these results with the binder testing results suggests that the embrittlement temperature of mastic/binder coated aggregates is lower than the embrittlement temperature of the binder itself. Several possibilities were hypothesized to explain the difference in embrittlement temperature measured in these three material configurations: 1) difference in temperature profiles (gradient across specimen); 2) differences in average ‘film thickness’; 3) difference in behavior at material interfaces in the three test configurations (granite-binder interface in binder testing; binder-coarse aggregate interface, and; binder-mastic-coarse aggregates interfaces), and; 4) geometry/constraint/size effects on fracture behavior. These differences suggest that the determination of embrittlement temperature will depend upon certain aspects testing configuration (such as temperature gradients and temperature probe location(s)) and material composition, and that variables such as these will need to be considered for standardization of mastic/mixture testing in order to normalize inter-laboratory test results.

**Table 5. Binder, Binder Coated Aggregate, and Mastic Coated Aggregate Test Results**

Sample ID	Replicate	Asphalt Binder			Binder Coated Aggregate			Mastic Coated Aggregate		
		AE Cracking Temp (°C)	Average	CoV%	AE Cracking Temp (°C)	Average	CoV%	AE Cracking Temp (°C)	Average	CoV%
TANK PG64-22	#1	-28.34			-33.12			-33.92		
	#2	-26.73	-27.5	2.9%	-30.78	-32.1	3.7%	-32.32	-32.7	3.4%
	#3	-27.42			-32.39			-31.81		
PAV PG64-22	#1	-23.91			-31.29			-32.48		
	#2	-25.07	-24.4	2.4%	-30.50	-30.6	2.1%	-29.89	-31.4	4.3%
	#3	-24.33			-30.03			-31.93		
TANK PG70-22	#1	-33.12			-37.48			-37.73		
	#2	-36.18	-34.7	4.4%	-38.31	-37.6	1.6%	-39.56	-38.8	2.4%
	#3	-34.70			-37.11			-38.98		
TANK AAD1	#1	-34.59			-40.12			-42.27		
	#2	-33.32	-34.6	3.6%	-41.50	-40.6	2.0%	-43.28	-41.6	4.9%
	#3	-35.83			-40.03			-39.37		
Sasobit-modified TANK- PG6422	#1	-28.73			-35.16			-33.62		
	#2	-27.92	-28.2	1.7%	-34.20	-34.6	1.5%	-38.33	-36.6	7.1%
	#3	-27.85			-34.30			-37.86		

### 3.2. AE Testing of Compacted Asphalt Mixtures

During the course of this study, the AE testing technique was utilized to evaluate the low temperature cracking performance of compacted asphalt mixtures. AE tests were conducted on lab-compacted gyratory mixtures from an ongoing Pooled Fund Low Temperature Cracking (LTC) study as well as field cores and lab compacted mixtures provided by the Asphalt Institute. Mixture samples were sliced to prepare semicircular, 50mm thick AE specimens. Specimens of 150 mm diameter semicircular shape with 50 mm thickness were prepared for AE testing. In the same manner as in binder testing, mixture specimens were positioned on a large metal plate inside an insulated cooling chamber surrounded by dry ice. The AE testing setup specimen dimensions are schematically shown in Figure 18(a) and (b), respectively.

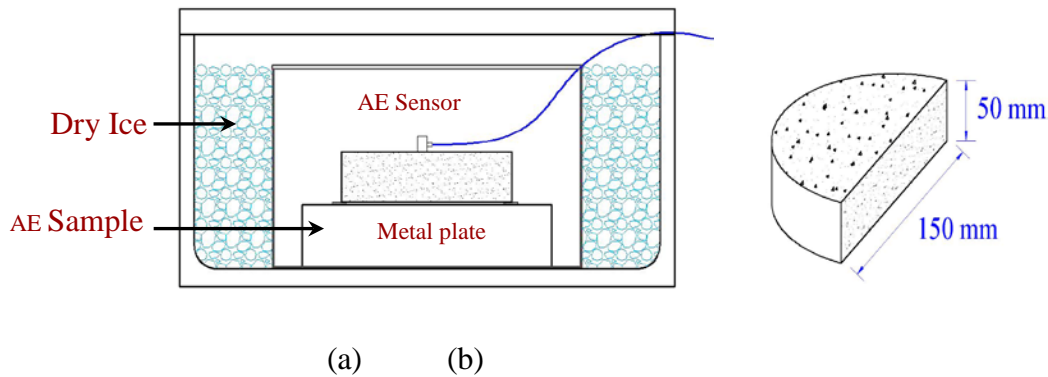


**Figure 18. (a) AE Testing Set-up (b) AE Testing Specimen [11]**

In addition to embrittlement temperature, testing results indicated that the temperature at which a maximum acoustic energy release is observed was a very repeatable parameter for the broad range of materials tested. Like embrittlement temperature, this quantity is also expected to be an intrinsic fracture property of the material. The concepts of embrittlement temperature ( $T_{EMB}$ ) and temperature of maximum AE event energy ( $T_{MAX}$ ) for asphalt mixtures are shown in Figure 19. The number of recorded AE events during the compacted mixture test is significantly higher than that observed during asphalt binder testing. The majority of these events are caused by microcracking resulting from asphalt mastic brittleness and the action of tensile thermal stresses within the material (Figure 20).

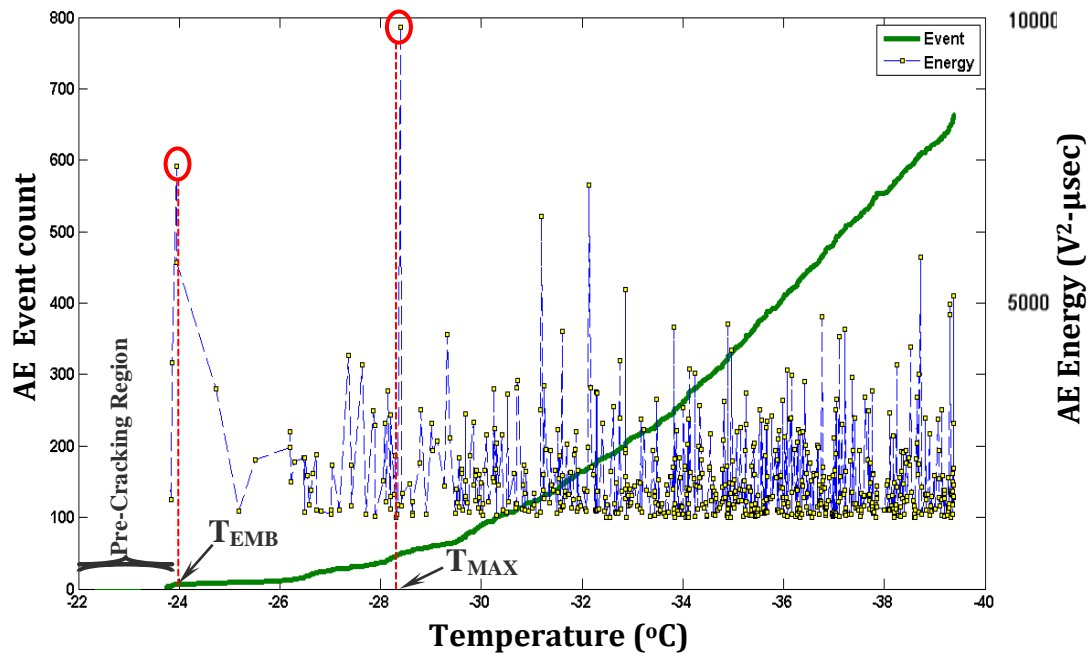


**Figure 19. Typical Plot of Event Count and AE Energy Versus Temperature**

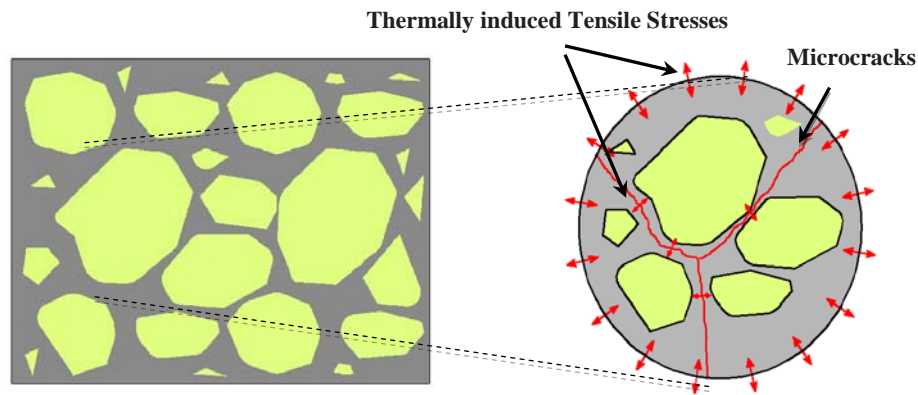


**Figure 20. Thermally Induced Stresses within the Asphalt Mastic[18]**

### **3.2.1 LTC Study Lab Compacted Asphalt Mixtures**

Acoustic emission tests were conducted for four mixtures from the LTC study, namely sections 20, 22 and 33, as reported in Table 6. Temperatures corresponding to the embrittlement temperature event (first major event) as well as the maximum energy event are shown. Notice that tests were conducted for mix specimens with 4 and 7% air void levels. The embrittlement temperature data indicates that for Sections 20 and 21 the onset of damage during rapid cooling begins at temperatures well above the Superpave PG low temperature of the virgin binder. This might be linked to the presence of 30% RAP in the mix,

whereby, the aged binder from RAP leads to increased brittleness and earlier onset of measured microcracking. On the other hand, the temperatures corresponding to the maximum energy events for Sections 20 and 21 seem to correspond to the PG low temperature (PGLT) grade of the virgin binder. Similar observations can be made for Section 22 where the first major acoustic event occurred at a temperature above the PGLT grade of the virgin binder, whereas the maximum acoustic energy was released at a temperature close to or lower than the virgin binder PGLT grade. The results for Section 33 follow similar trends as the other sections, where the embrittlement temperature is higher than that of the PGLT grade of the virgin binder, whereas the temperature at maximum energy release is similar to the PGLT. The air void level did not reveal a specific trend in either the embrittlement temperature or the temperature corresponding to the maximum energy event. This is expected, as the acoustic activity is measure of fracture and fracture phase change for the mastic portion of the mixture. In addition, the 4 and 7% air void levels were targeted for 180 mm tall gyratory specimens, while AE testing was performed on 50 mm thick samples, which almost certainly had lower air void levels and possibly less difference in air void level between the two groups.

**Table 6. Acoustic Emissions Test Results (Embrittlement Temperature and Temperature at Maximum Energy Event)**

Sample ID	Air Void %	Replicate	Embrittlement Temperature			Temp. at Max. Energy Event		T <sub>Max</sub>
			T <sub>Emb</sub> (°C)			Energy Event (°C)		
			T <sub>Emb</sub>	Average	CoV	T <sub>MEE</sub>	Average	
Section 20 (PG58-28) 30%RAP	4%	#1	-17.45			-29.97		
		#2	-21.36	-19.45	9.74%	-29.69	-30.06	1.40%
		#3	-18.25			-29.90		
		#4	-20.75			-30.66		
	7%	#1	-24.10			-29.92		
		#2	-22.87	-24.65	8.66%	-28.04	-30.26	6.24%
		#3	-27.75			-30.44		
		#4	-23.89			-32.63		
Section 21 (PG58-28) 30%RAP	4%	#1	-21.00			-29.74		
		#2	-21.29	-22.24	8.55%	-32.66	-31.89	5.92%
		#3	-24.43			-33.27		
	7%	#1	-19.90			-26.82		
		#2	-21.59	-20.91	4.27%	-29.85	-28.28	5.37%
		#3	-21.24			-28.16		
Section 22 (PG58-34) 30%RAP	4%	#1	-28.05			-32.02		
		#2	-29.35	-28.75	8.18%	-35.50	-33.70	4.27%
		#3	-31.61			-33.38		
		#4	-26.00			-33.89		
	7%	#1	-29.86			-35.74		
		#2	-28.33	-29.90	4.73%	-37.84	-36.97	2.71%
		#3	-29.64			-37.73		
		#4	-31.76			-36.57		

<b>Section 33 (PG58-34)</b>	<b>4%</b>	#1	-30.40			-31.20	
		#2	-28.16	<b>-30.50</b>	5.54%	-28.85	<b>-31.16</b> 5.24%
		#3	-31.46			-32.03	
		#4	-31.97			-32.54	
	<b>7%</b>	#1	-29.87			-32.94	
		#2	-30.74	<b>-29.73</b>	2.69%	-31.02	<b>-33.02</b> 4.33%
		#3	-29.48			-34.12	
		#4	-28.83			-33.98	

### 3.2.2 Asphalt Institute Compacted Asphalt Mixtures:

AE tests were conducted on several lab compacted asphalt mixtures as well as field cores provided by the Asphalt Institute, which were part of a study investigating non-load associated cracking in airfield pavements [19]. Three sets of lab compacted mixtures at three different aging levels including: 0, 4 and 24 hours were tested. All aging was performed on loose mixture before compaction to expedite and simplify the lab conditioning process. According to information provided by the Asphalt Institute, three asphalt binders namely, Gulf-Southeast (PG64-22), Western Canadian (PG64-28) and West Texas sour (PG64-16), were utilized in the study mixtures. The asphalt binders possessed different low temperature relaxation properties as defined by the BBR m-value. Table 7 summarizes the lab compacted AE test results. It is observed that for all samples at different aging levels, the more aged the sample, the warmer the  $T_{EMB}$  of that material. It was hypothesized that aging causes a significant loss in relaxation properties of the asphalt mastic at lower temperatures, and this change results in deteriorating fracture cracking resistance of the material. Similar to LTC mixtures, for all lab compacted samples, the  $T_{EMB}$  is warmer than the PGLT of virgin binder, whereas for most cases the maximum acoustic energy temperatures ( $T_{Max}$ ) is close to virgin binder's PGLT [19].

In addition to lab compacted samples, several field cores provided by Asphalt Institute were tested to assess their low temperature cracking behavior using AE technique. Field cores obtained from three different projects located at different regions with different climates as well as different asphalt crude sources.. Coring locations on General Aviation (GA) pavements were Montana and New Mexico. These locations are shown in Figure 21, while typical photos of cores are provided in Figure 22. The coring location selected with the goal to obtain cores from both cracked and non-cracked sections. The locations selected were matched to the binder source wherever possible. For example, it was believed that the Montana airport cores would reflect an asphalt source similar to the Western Canadian crude, whereas the New Mexico sites would more likely resemble asphalt as refined from the West Texas Sour crude.



**Table 7. Acoustic Emissions Test Results of Lab Compacted Mixtures**

Sample ID	Aging Level	T <sub>Emb</sub> (°C)		T <sub>Max Energy Event</sub> (°C)	
		T <sub>Emb</sub> (°C)	CoV%	T <sub>Max Energy Event</sub> (°C)	CoV%
Gulf South East Crude (PG64-22)	0 Hrs	-18.00	1.26%	-21.71	2.18%
	4 Hrs	-16.99	7.37%	-21.90	8.07%
	24 Hr	-13.96	9.17%	-20.50	7.49%
Western Canadian Crude (PG64-28)	0 Hrs	-22.84	8.70%	-27.82	7.80%
	4 Hrs	-20.67	1.27%	-27.78	2.80%
	24 Hr	-16.37	10.07%	-22.16	7.47%
Western Texas Sour Crude (PG 64-16)	0 Hrs	-12.55	4.68%	-23.49	2.89%
	4 Hrs	-10.03	4.09%	-21.71	6.42%
	24 Hr	-8.42	12.93%	-18.13	6.32%

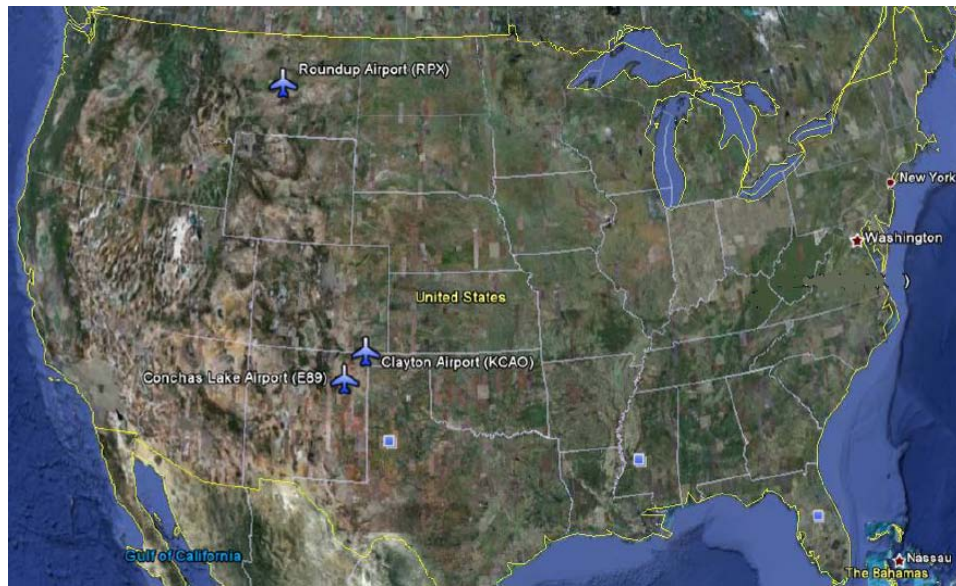


**Figure 21. Coring Site Locations: New Mexico, Montana [19].**



**Figure 22. Sample Cores from Rounup, MT and Conchas Lake, NM[19].**

Cores were taken from airports representing in-service pavements. In Montana, cores were taken from one airport – identified as Roundup – that had recently received an overlay of an older, cracked pavement. The estimated age of the pavement is 12 to 15 years old. A number of cracks were present in this pavement, which have been previously routed and sealed. Obtained cores were split into layers with the upper layer representing the new pavement (Roundup Top) and the lower layer representing the older pavement (Roundup Bottom). In New Mexico, cores were taken from the Clayton airport and the Conchas Lake airport. Site reports for the Clayton airport indicate that it was paved in 2004. Some low severity longitudinal cracking and raveling was identified. The Conchas airfield was paved in 2001. Site reports from the Conchas Lake airport indicate that some moderate severity distresses were identified over most of the paved area, and that the pavement had a weathered appearance [19].

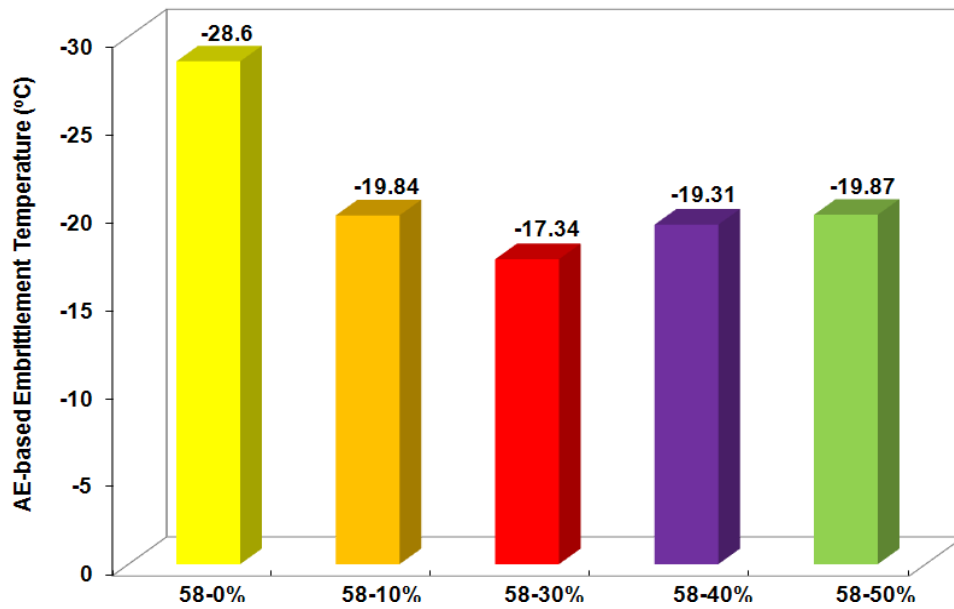
Obtained AE test results of provided field cores are presented in Table 8. The Embrittlement temperature of field cores matches with the reported cracking condition of the airfields. Both Conchas and Clayton airfields are paved using Western Canadian Crude asphalt binder. It is seen that  $T_{EMB}$  of Conchas samples is much higher than Clayton samples. This can be attributed to the fact that Conchas pavement encountered more severe age hardening, as the pavement appears slightly oxidized already in the field compared to Clayton pavement which was reported to be in good condition. For Roundup samples, as expected, the Roundup Top samples which belong to the newly paved overlay have better  $T_{EMB}$  as compared to the Roundup Bottom samples which are from the old pavement. For both Roundup pavement layers, which experience thermal cracking during service life, poor field aged embrittlement temperatures were measured (in the -12 to -13 C range). It is noted that the COV values for the bottom of the pavement were significantly lower than the top of the pavement, indicating more consistency in the physical properties between core samples for the Roundup bottom samples.

**Table 8. Acoustic Emissions Test Results of Asphalt Institute Field Cores**

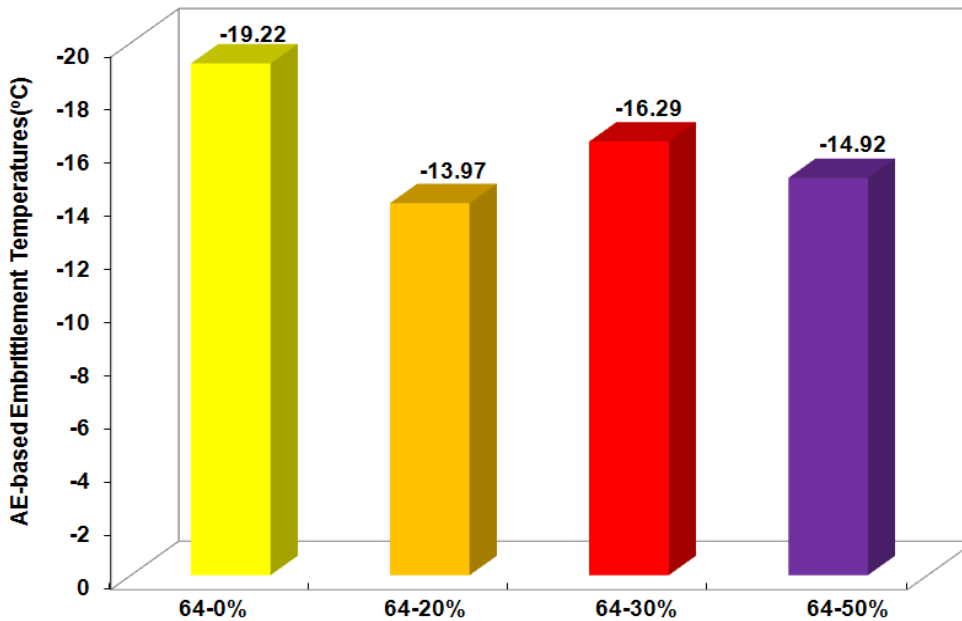
Sample ID	$T_{Emb}$ (°C)		$T_{Max}$ Energy Event (°C)	
	$T_{Emb}$ (°C)	CoV%	$T_{Max}$ Energy Event (°C)	CoV%
<b>Conchas Lake Airport, NM</b>	<b>-12.65</b>	4.92%	<b>-27.64</b>	1.77%
<b>Clayton Airport, NM</b>	<b>-21.57</b>	10.10%	<b>-29.72</b>	1.38%
<b>Roundup Top, MT</b>	<b>-13.02</b>	17.33%	<b>-26.06</b>	4.91%
<b>Roundup Bottom, MT</b>	<b>-12.17</b>	0.17%	<b>-23.27</b>	2.52%

### ***3.2.3 Mixtures Containing Recycled Asphalt Pavement (RAP)***

The amount of RAP usage in asphalt pavements has been escalating significantly in recent years. The two primary motivational forces behind the utilization of RAP are cost savings and environmental benefits. In this study, in order to investigate the effects of adding RAP on embrittlement temperature of asphalt mixtures a 19-mm nominal maximum aggregate size mix with a target asphalt content of 5.9% and 0% - 50% RAP by total weight of mixture was tested. AE tests were conducted on various asphalt mixtures, namely: two control mixtures with no RAP, manufactured with PG 64-22 and PG 58-28 asphalt binders; and seven mixtures containing 0-50% RAP manufactured using PG 64-22 and PG 58-28 for the virgin binder (Figure 23 [20]).



(a) PG 58-28 Mixtures



(b) PG 64-22 Mixtures

**Figure 23. Embrittlement Temperature of RAP Mixtures Determined Using AE[20]**

As expected, the embrittlement temperature of mixtures containing RAP was found to be higher than the control mixture with 0% RAP. It appears that the acoustic emission technique is able to detect the presence and, to some extent, the effect of the RAP in an asphalt mixture. The results obtained suggest that there may have been limited mixing between the virgin binder and RAP binder in these specimens, as

the embrittlement temperature did not vary significantly between the various amounts of RAP in the mixture. Instead, it can be hypothesized that the results indicate that the embrittlement point of the most brittle fraction of the asphalt mastic was in fact measured, which would be the unmixed RAP binder existing in the mixture. As expected, the RAP had more of an effect on the mixture containing the softer virgin binder. These findings suggest that the AE test could possibly be used as a method to determine if RAP was present in an HMA mixture for quality control purposes. Additional work is underway to determine if further signal analysis can yield predictions of RAP amount and/or information regarding the degree of blending of virgin and recycled asphalt binder in mixtures containing RAP.

#### 4. IMPROVED COOLING DEVICE

Developing an improved cooling system suitable to use for both binder and mixture AE-based test was one of the proposed research tasks. During the course. In order to accomplish this purpose several available options have been examined. As a result two cooling systems namely, thermoelectric cooler and Shuttle portable ULT freezer, are introduced.

##### 4.1. Thermoelectric Cooling System (TEC)

In recent years, the use of thermoelectric-type cooling devices has increased significantly. This technology is well-suited for a wide variety of applications because of inherent advantages such as high-flux spot-cooling capability, low maintenance requirements, fast response, and lack of mechanical vibrations, and because of its compact structure. Thermoelectric coolers (TEC) are energy conversion devices that use electrical energy to provide cooling capability based on the Peltier effect. The Peltier effect takes place when an electric current flows across a junction of two different semiconductor materials. Heat will be generated or absorbed at the junction at a constant rate. Whether heat is absorbed or generated at the junction depends on the direction of current flow. The heat generation rate is directly proportional to the current and changes sign if the current changes sign [21, 22].

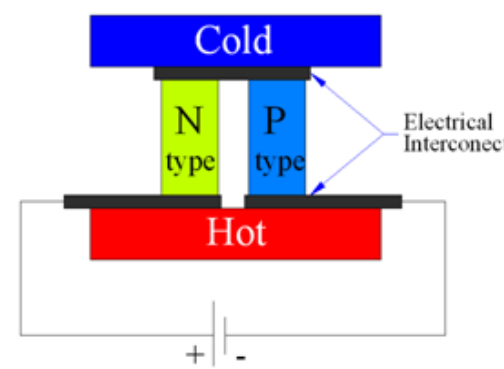


**Figure 24. A Typical Thermoelectric Cooling Unit**

Figure 24 shows a typical thermoelectric cooling unit, where electric current flows through the N-type element, crosses a metallic interconnect, and passes into the P-type element. Electrons in the N-type element will flow opposite of the direction of current and in the P-type element will flow in the direction of current, both removing heat from top surface of the device. The combination of many pairs of P and N-semiconductors allows the creation of thermoelectric cooling plates of relatively high power (Figure 25),

which form P-N- and N-P-junctions. Each junction has a thermal contact with both cold and hot sides of a TEC [21, 22].

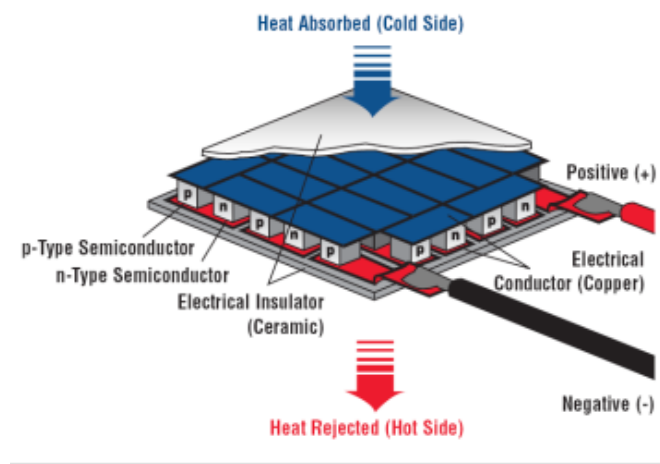


**Figure 25. Usage of Combination of P- and N-type Semiconductors in Thermoelectric Coolers**

During the course of this study, a thermoelectric-based cooling system was designed and tested. The prototype was designed with significant assistance from Test Quip, Inc., and TE Technology, Inc. The Peltier thermoelectric cooling (TEC) device was thought to be a low-cost, small footprint option for programmable cooling in the proposed AE test. Another goal was to develop a cooling system with the ability to test a wide variety of binders from around the US, especially binders utilized in very cold regions such as Minnesota and North Dakota. This required the TEC device to have the ability to cool to -50C. A TEC module provides a temperature difference of several tens of degrees Celsius, rendering a single unit as insufficient for this application. With forced cooling of the hot surface, a two-staged Peltier system can reach temperatures below 0 Celsius. To achieve a larger temperature differential, a cascade configuration was designed. To achieve -50C cooling, a 4-stage Peltier cooler (Model CP-3213) with input power of 288 W (48 V, 6 A) was designed. Figure 26 schematically shows the 4-stage Peltier TEC device as well as the prepared plastic cooling chamber mounted on top of the TEC device.

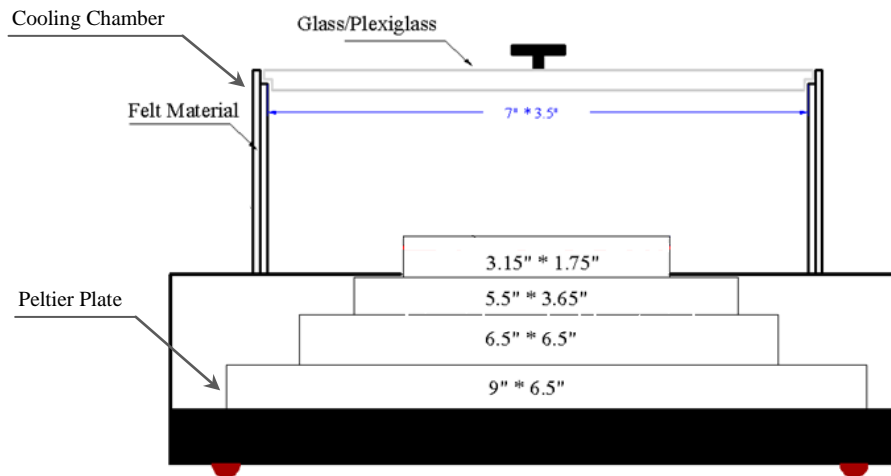


**Figure 26. 4-Stage Peltier TEC Device with Cooling Chamber**

The main components of the TEC device including the 4-stage Peltier device, cooling chamber, temperature controller and the power supply are shown in Figure 27. The TC-48-20 thermoelectric temperature controller, housed in a die-cast aluminum box, capable of controlling up to 50 volts and 20 amps was used in the TEC system. The liquid crystal display capable of displaying two lines of text, each up to 16 characters long allows the user to monitor the sensor temperature, output level, and menu settings. Moreover, it allows the user to adjust all of the basic controller parameters such as the set temperature, tuning parameters, and alarm parameters. The controller is connected to a computer via RS232 port for more advanced program control, data graphing, and data logging. All of the controller parameters, including some of the advanced parameters which are not adjustable through the onboard menu, can be adjusted via the temperature controller software.

Temperature was monitored by locating the thermistor at the cold side of the top Peltier plate inside the cooling chamber. At least 50mm of the thermistor wire was thermally connected to the cold plate in order to achieve better control stability. The controller does not have an internal fuse or circuitry to limit current. Therefore, a power supply with integral over current protection was used to protect the controller/TE device. Although it is anticipated that the standard AE test method will involve a linear rate of cooling, the TEC device is capable of versatile computer-controlled cooling, allowing effects of temperature cycling and low temperature physical hardening to be explored. The hook up diagram of the TEC system is presented in Figure 28.

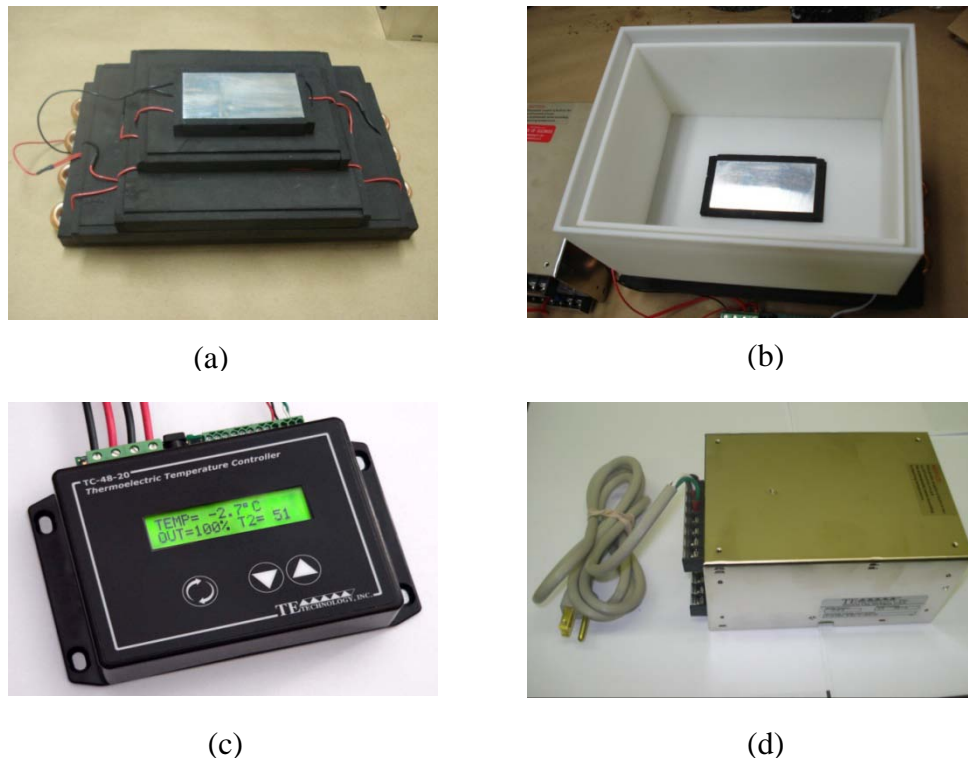


**Figure 27. TEC System Main Components: (a) 4-Stage Peltier TEC, (b) Cooling Chamber, (c) Temperature Controller (d) Power Supply**



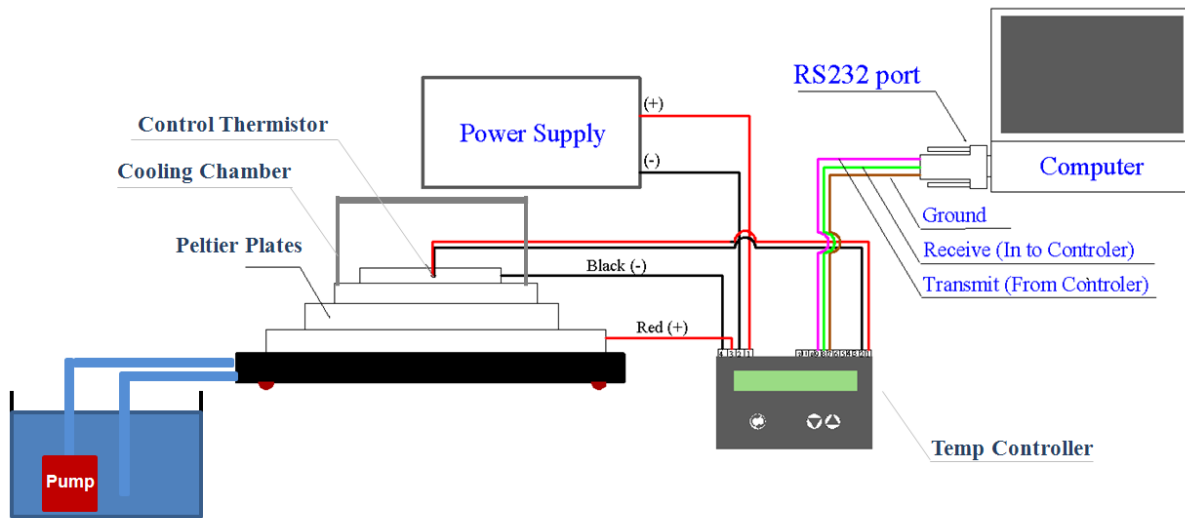


**Figure 28. TEC system Wiring Diagram**

Reaching  $-50^{\circ}\text{C}$  requires approximately 6 W of heat pumping to overcome passive heat loads, which was very difficult to achieve using a fan-cooled heat sink. Instead, a liquid-cooled heat sink was determined to be necessary, with an approximate flow rate of 3.2 L/min (50 gallon/hr), providing 7 W of cooling at  $-50^{\circ}\text{C}$ . The designed TEC device was used in AE testing of asphalt binder and asphalt mixture tests, as shown in Figure 29.



**Figure 29. TEC Device : (a) AE Asphalt Binder Test (b) AE Mixture Test**

The TEC-based cascade cooling device and associated cooling chamber was designed, assembled, and initially tested towards the end of this project. Although only preliminary results have been obtained at the time of this writing, the technology appears to be promising. The manufacturer (TE Technology, Inc.), who was also responsible for the design of the cascade system, successfully bench tested the device to



provide linear cooling down to -50C. A limiting factor preventing the standardization of this method of cooling during this project was the lack of a cold water source in the non-destructive testing and evaluation (NDE) laboratory at the University of Illinois, and insufficient time and funding to relocate the test during the course of this study or to install a water and drain system in the NDE lab. Instead, a large water tank with a circulating pump was installed in the NDE laboratory to conduct preliminary field testing of the TEC cooling system. The device was found to provide linear cooling down to about -15C, after which the temperature of the water in the cooling bath was elevated to the point where no further cooling was possible. Although further testing is underway to fully evaluate the feasibility of the TEC-based system as an efficient means for providing linear cooling in the AE test, the method indeed appears to be promising. The hardware cost for the cascade system is approximately \$2000.00, and considering the cost of the cooling chamber, temperature controller, etc., the entire TEC-based system is expected to cost less than \$3000.00. This is very competitive as compared to conventional cooling systems, which can exceed two or even three times this cost when providing air cooling to -50C. The main disadvantage of the current TEC-based system is its reliance on a cold water source, and the environmental impact and cost of this cold water source. For testing of specimens requiring less cooling, the cold water option may not be needed. In addition, further cascading of TEC plates, combined with air cooling, may serve as a future alternative to the water-cooled configuration. It is expected that future advances in TEC-type cooling plates and related technologies will result in the increased usage of these systems in low temperature testing devices in the future, due to their small form factor, quiet operation, and low maintenance requirements. In our assessment, these systems have the capability to provide the needed cooling capacity for small binder and mixture specimens at the present time, and the cooling of larger mix specimens is a distinct possibility as the efficiency and power of these systems is improved in the future.

#### **4.1. Shuttle ULT-25 Portable Freezer**

The Shuttle ULT-25 (Figure 30) is a portable freezer, capable of rapidly cooling to an astonishingly low temperature of -86°C. It is lightweight and easily transported, designed to operate on both AC and DC power at both 60Hz and 50Hz electrical systems. It is also very quiet and energy-efficient (150 watts maximum energy consumption rate during steady state operation). It is designed to be placed on a desktop, lab bench or cart in laboratories or operating rooms, and is easily transferred to vehicles, aircraft, and remote and disaster locations. Currently, the Shuttle cooling system is mainly being used within the medical research community, for pharmaceutical distribution, and for geological and archeological specimen transport and storage [23].

The Shuttle ULT-25 cooling system operates independently for up to two hours when connected to an optional uninterruptible power supply, and can operate from a standard car or truck battery supply through the vehicle DC power adapter supplied with the unit. The shuttle ULT cooling system is lightweight, weighing 40 lbs (18 kg) empty, and its cooling chamber holds a volume of 0.9 ft<sup>3</sup> (25 liters). Its interior and exterior dimensions are 13.0" L x 8.7" W x 13.0" D (330.2 x 222.2 x 330.2mm) and 27.1" L x 13.6" W x 18.3" H (688.1 x 346.5 x 464.3mm), respectively. The self-modulating cooling system demands around 230 watts at ambient startup and decreases through initial pull down to a steady state of 150 watts. There is an access port of 1/4" (6.3mm) diameter is provided on one side of the device, which was used in our application for thermocouple and AE piezoelectric sensor cable throughput [23].



(a)



(b)

**Figure 30. (a) Shuttle ULT-25 portable Freezer (b) Inside of ULT-25: The Cooling Chamber [23]**

The Shuttle ULT-25 cooling system employs free-piston Stirling engine technology that uses a micro-fluid cooling media to eliminate conventional refrigeration or cascade compressor systems. This cooling system operates without noisy refrigeration compressors or costly cascade systems associated with ultra-low temperature storage. Free-piston Stirling technology is quite simple in design, featuring a thermosiphon that contains no moving parts, which is integrated into a rugged, lightweight cabinet with weatherproof electronic controls. The Stirling technology is a proven, dependable, maintenance-free heat transfer process that is widely used in aerospace, energy and military applications for cooling and power generation [23].

The free-piston Stirling engine is schematically illustrated in Figure 31. This engine contains two moving parts that float on helium gas bearings to eliminate contact wear. Freezing is performed by continuous evaporation and condensation of the cooling medium permanently sealed within the thermosiphon where ultra-low temperature is constant from top to bottom.

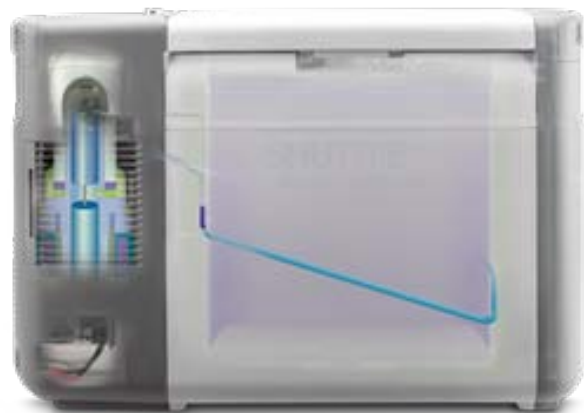
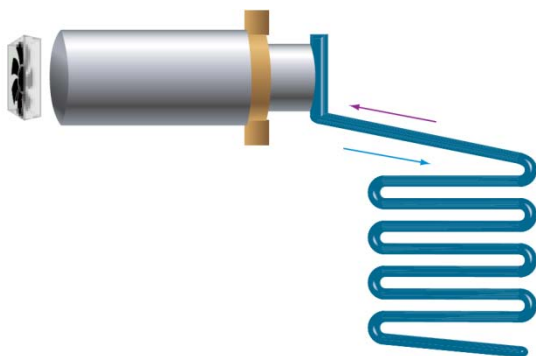


**Figure 31. The Free-piston Stirling Engine [23]**

Unlike conventional refrigeration systems that cycle on and off, the free piston Stirling system operates continuously and modulates cooling capacity on demand to maximize temperature uniformity within the chamber. The thermosiphon evaporator operates on a microcharge cooling medium of 0.3 oz to 0.6 oz (9 to 18 grams) depending on the medium used. The system contains no compressors or lubricating oils. The operating characteristics of a conventional refrigeration system and a free piston Stirling system are schematically shown and compared in Figure 32. Since there is no on/off cycling in free piston Stirling system it is seen that component wear and energy spikes common to start/stop cycling is virtually eliminated, creating and maintaining a steady-state temperature at the desired setpoint without a sawtooth curve common to conventional refrigeration systems [23].

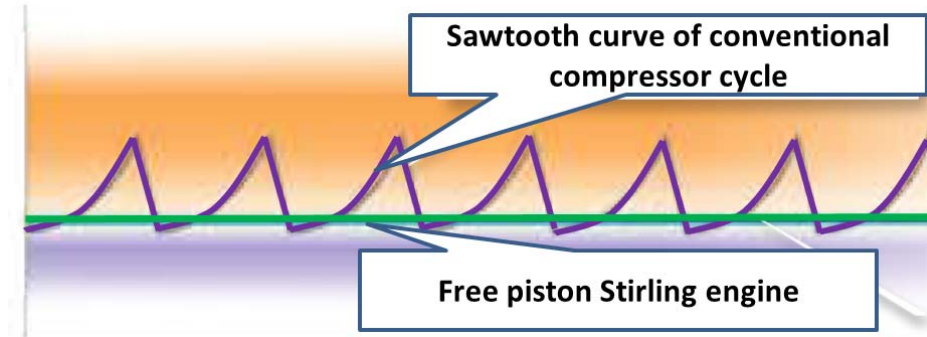


**Figure 32. Comparison between Free-piston Stirling Engine vs. Conventional Refrigeration systems**

Toward the end of this study, the Shuttle cooling system enabled us to apply different linear cooling rates and to investigate cooling rate effects on the low temperature behavior of asphalt materials. In order to simulate a linear cooling rate, portable freezer set temperature was reduced  $10^{\circ}\text{C}$  at various selected time intervals, denoted as 't', where ( $1^{\circ}\text{C}/\text{min}$ :  $t=10$  min,  $0.67^{\circ}\text{C}/\text{min}$ :  $t=15$  min,  $0.34^{\circ}\text{C}/\text{min}$ :  $t=30$  min,  $0.2^{\circ}\text{C}/\text{min}$ :  $t=50$  min). Figure 33 schematically shows a typical portable freezer set temperature profile. Cooling chamber air temperature as well as temperature at the surface of AE sample was recorded using two thermocouples.

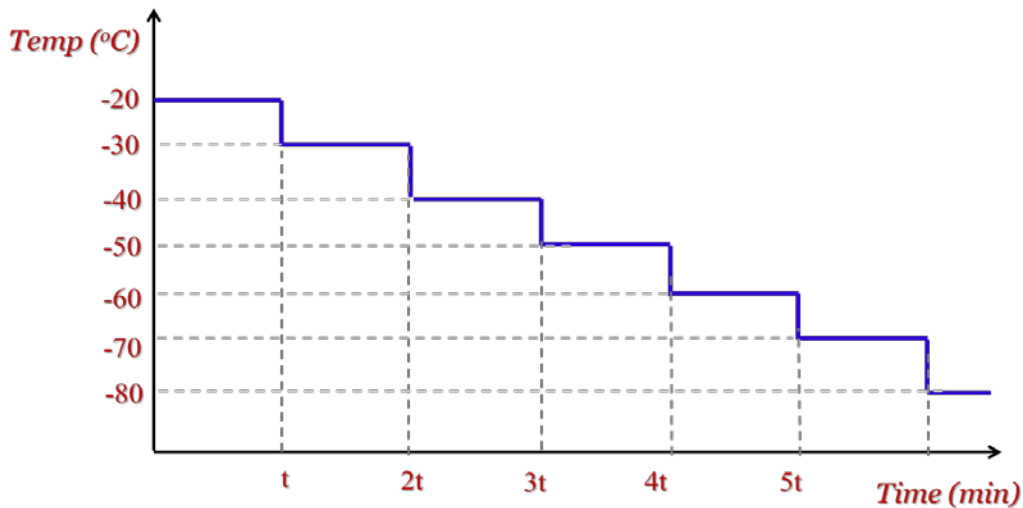


**Figure 33. Shuttle Portable Freezer Set Temperature Profile**

A typical linear thermal gradient as measured in the asphalt binder sample along with cooling chamber air temperature for an average applied cooling rate of 1°C/min are illustrated in Figure 34 . It was observed that the measured linear cooling rate of AE sample was not necessarily the same as the average applied cooling rate of the portable freezer. Examining different linear cooling rates showed that the lower the average applied cooling rate, the lower the difference between AE sample and portable freezer cooling rates. For instance, in the case of an average cooling rate of 1°C/min, the asphalt sample cooled at a rate that was 30% slower than the applied cooling rate (0.0117 °C/sec = 0.7 °C/min), whereas when the applied cooling rate was slowed down to 0.34 °C/min, the asphalt sample cooling rate was virtually identical to the freezer cooling rate. These results are presented in Figure 35.

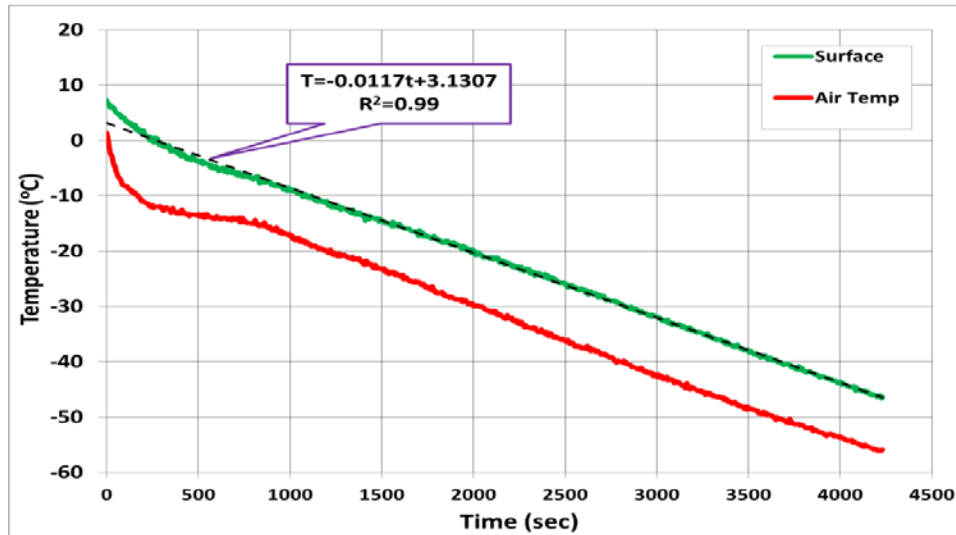


**Figure 34. Typical Linear Thermal Gradient of AE Sample for Average Applied Cooling Rate of 1°C/min**

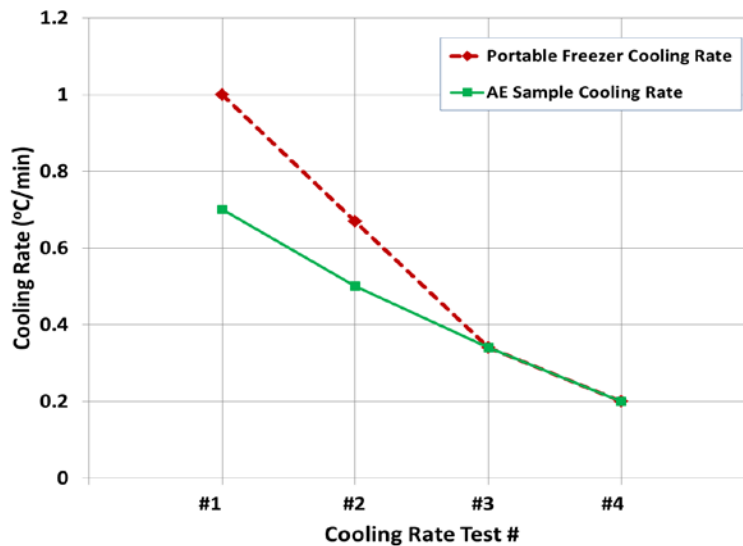


**Figure 35. Different Applied and Measured Cooling Rates for Freezer and AE Sample.**

Effects of different linear cooling rates on AE embrittlement and max energy event temperature parameters were investigated. AE-based tests were conducted on three asphalt binders namely, TANK PG64-22, TANK AAG1(PG58-16) and RTFO AAG1(PG 58-16). Tables 9,10 and 11 summarize the results obtained for unaged PG 64-22, and for unaged and short term aged PG 58-16 binders, respectively. The results obtained  $T_{EMB}$  is not affected by cooling rate within this range. Similarly,  $T_{MAX}$  was found to be relatively unaffected by cooling rate within this range. From these results, we conclude that a 1°C/min cooling rate would provide a practical testing protocol. However, it will be necessary to monitor the temperature within the specimen (or at the surface of the specimen) in order to account for the difference between chamber and sample temperature at this cooling rate.

**Table 9. AE Test Results of TANK PG64-22 at Different Cooling Rates**

Sample ID	Cooling Rate	Replicate	$T_{Emb}$ (°C)			$T_{Max}$ Energy Event (°C)		
			$T_{Emb}$ (°C)	Average	CoV%	$T_{Max}$ Energy Event (°C)	Average	CoV%
TANK-PG64-22	Linear Cooling 1°C/Min	#1	-25.70	<b>-27.29</b>	5.41%	-30.08	<b>-30.15</b>	0.42%
		#2	-28.62			-30.30		
		#3	-27.54			-30.08		
	Linear Cooling 0.67°C/Min	#1	-26.80	<b>-27.70</b>	2.96%	-30.22	<b>-30.21</b>	0.58%
		#2	-27.90			-30.03		
		#3	-28.40			-30.38		
	Linear Cooling 0.34°C/Min	#1	-28.01	<b>-27.55</b>	1.64%	-29.91	<b>-30.24</b>	1.50%
		#2	-27.11			-30.76		
		#3	-27.52			-30.06		
	Linear Cooling 0.2°C/Min	#1	-27.91	<b>-27.82</b>	2.21%	-30.21	<b>-30.12</b>	1.48%
		#2	-27.17			-29.64		
		#3	-28.39			-30.52		

**Table 10. AE Test Results of TANK AAG1(PG58-16) at Different Cooling Rates**

Sample ID	Cooling Rate	Replicate	T <sub>Emb</sub> (°C)			T <sub>Max Energy Event</sub> (°C)		
			T <sub>Emb</sub> (°C)	Average	CoV%	T <sub>Max Energy Event</sub> (°C)	Average	CoV%
TANK-AAG1	Linear Cooling 1°C/Min	#1	-19.98	<b>-19.67</b>	2.89%	-23.13	<b>-22.14</b>	3.87%
		#2	-20.01			-21.62		
		#3	-19.01			-21.67		
	Linear Cooling 0.67°C/Min	#1	-20.01	<b>-20.26</b>	4.00%	-23.27	<b>-22.02</b>	4.93%
		#2	-19.61			-21.29		
		#3	-21.17			-21.51		
	Linear Cooling 0.34°C/Min	#1	-20.92	<b>-20.40</b>	2.55%	-21.94	<b>-22.05</b>	2.71%
		#2	-20.39			-22.69		
		#3	-19.88			-21.51		
	Linear Cooling 0.2°C/Min	#1	-20.62	<b>-20.45</b>	1.81%	-22.94	<b>-22.08</b>	3.41%
		#2	-20.71			-21.52		
		#3	-20.03			-21.79		

**Table 11. AE Test Results of RTFO AAG1(PG58-16) at Different Cooling Rates**

Sample ID	Cooling Rate	Replicate	T <sub>Emb</sub> (°C)			T <sub>Max Energy Event</sub> (°C)		
			T <sub>Emb</sub> (°C)	Average	CoV%	T <sub>Max Energy Event</sub> (°C)	Average	CoV%
RTFO AAG1	Linear Cooling 1°C/Min	#1	-16.64	<b>-18.27</b>	7.93%	-21.80	<b>-21.47</b>	3.05%
		#2	-19.41			-20.72		
		#3	-18.76			-21.90		
	Linear Cooling 0.67°C/Min	#1	-19.02	<b>-20.38</b>	6.80%	-22.58	<b>-21.97</b>	2.87%
		#2	-20.34			-21.32		
		#3	-21.79			-22.01		
	Linear Cooling 0.34°C/Min	#1	-19.07	<b>-19.84</b>	5.30%	-21.32	<b>-21.56</b>	1.19%
		#2	-21.04			-21.83		
		#3	-19.42			-21.52		
	Linear Cooling 0.2°C/Min	#1	-20.43	<b>-19.96</b>	2.92%	-21.93	<b>-21.68</b>	1.62%
		#2	-19.31			-21.28		
		#3	-20.15			-21.84		

## 5. CONCLUSIONS

NCHRP Project #144 involved research aimed at improving and standardizing the Acoustic Emissions technique as a rapid and practical testing method to assess the low temperature cracking behavior of asphalt binder mixtures. During the course of this study, AE tests were conducted to evaluate the concept of an embrittlement temperature through the testing of a wide range of asphalt binders and mixtures, including lab and field specimens. The temperature corresponding to the first major acoustic emission event, as determined using a standardized signal analysis technique, is now defined as the embrittlement temperature. For asphalt binders, it was observed that AE test results are sensitive to binder type and aging level. The repeatability of the AE testing technique was improved during the course of this study, and was found to be as good as or better than other lower temperature binder tests currently in use. Predictions of critical cracking temperatures obtained from BBR testing were found to be in close agreement with AE predictions, and very highly correlated.

An important aspect of this investigation was the extension of the AE test method to asphalt mixture testing, which opens the door for the use of the technique for pavement condition assessment. AE tests were performed on lab compacted mixtures provided by the Asphalt Institute and a pooled fund study on low temperature cracking. Characterization was performed to identify the embrittlement temperature and the temperature corresponding to the maximum acoustic event. Both of these temperatures are thought to represent fundamental thresholds in material behavior. It was observed that the AE technique is sensitive to aging level and binder grade in the of the asphalt mixtures. The embrittlement temperature was found to be a good indicator of the extent of damage which happens in the field, as the  $T_{EMB}$  results of the provided field cores matched well with the pavement condition as reported in the non-load associated cracking study for airfield pavements conducted by Asphalt Institute.

These results study suggest that the AE-based embrittlement temperature test may be a rapid, yet powerful tool for the characterization of low temperature behavior of asphalt binders and mixtures for material formulation, selection, design, and QC/QA. This method shows excellent promise as a tool to enhance pavement sustainability by allowing precise characterization of pavement surfaces, which can then be used to accurately program preventive maintenance and rehabilitation.

In addition to development of AE-based testing technique, an integrated thermoelectric-based cooling system (TEC) was developed during the course of this study. The improved prototype consists of a 4-stage Peltier cooler (Model CP-3213) with a liquid-cooled heat sink which is capable of reaching  $-50^{\circ}\text{C}$ . The TEC device is compact, requires little maintenance and is capable of versatile computer controlled cooling. It has the capacity to test a wide range of binders and mixtures, including binders utilized in very cold regions. However, more work is still needed to validate the TEC-based system for use with larger mixture specimens, as testing to date was only successfully carried out for binder specimens and relatively small (several centimeter sized) mixture specimens. A Stirling-engine based cooling system (Shuttle ULT-25) was also investigated, and found to produce excellent results. This quiet and efficient cooling system was far more powerful than the cascade thermoelectric cooling device, and was capable of reaching much lower temperatures (as low as  $-86^{\circ}\text{C}$ ). The current limitation of the Shuttle system is its inability to directly set a linear cooling rate. However, this can be overcome through manual operation, or in the future by modifying the temperature control system on the unit.

The work conducted under this NCHRP IDEA project has successfully positioned the proposed AE-based testing method as a market-ready, and practitioner-friendly technology based upon the following accomplishments: 1) the scientific basis for the material parameters measured in the proposed test, namely, the embrittlement temperature and max event energy temperature, have been solidly supported through lab and field sample testing and comparison to existing test methods; 2) the repeatability of the proposed method is very good, and at par or better than existing comparable low temperature asphalt binder and mixture tests; 3) the proposed test methods was shown to be versatile, with the capability to

test binder, mastic, and mixture specimens, and lab and field specimens; 4) the device has the ability to detect the presence of recycled asphalt pavement (RAP) in an asphalt mixture sample, which may be useful for quality assurance testing; 5) in addition to the embrittlement temperature and temperature of maximum energy event, the device has the potential to produce other cracking information, such as: event count, event energy, and spectral (frequency) information associated with recorded acoustic emission activities, which may lead to further uses of the device in material design and forensic applications; 6) field validation of the technique showed excellent promise for using the tool to assess current pavement condition from the standpoint of low temperature crack resistance, and; 7) the compact nature of the device appears to be enhanced by the availability and applicability of modern cooling devices such as thermoelectric-based systems. Based upon these findings, we conclude that the device is ready for commercial development at this time. Of course, the testing of additional material types including other available sustainable asphalt material technologies (e.g., other than the warm mix technologies tested herein) and further field validation studies are recommended to further validate the proposed testing method and to further broaden its range of applicability. Furthermore, the development of a standardized test method to be submitted to AASHTO is recommended and will be pursued soon.



## REFERENCES

1. Behnia, B., Buttlar, W.G., Apeagyei, A.K., and Reis, H. ."Determining the embrittlement temperature of asphalt binders using an acoustic emission approach," NDE/NDT for Highways and Bridges: Structural Materials Technology (SMT), New York, 2010
2. Apeagyei, A.K., Buttlar, W.G., and Reis, H., "Estimation of low-temperature embrittlement for asphalt binders using an acoustic emission approach" In INSIGHT—Nondestructive Testing and Condition Monitoring, The Journal of the British Institute for Non-Destructive Testing, 51(3), pp.129-136., 2009.
3. Kim, Y. R. "Modeling of Asphalt Concrete", McGraw-Hill, ASCE Press, 20084.
4. Hellier, C. J., "Handbook of Nondestructive Evaluation," McGraw-Hill, United States, ISBN 978-0-070-2812-19., 2001
5. Grosse, C.U, and Ohtsu, M., "Acoustic Emission Testing: Basics for Research- Applications in Civil Engineering," Springer, 2008.
6. Mix, P.E , "Introduction to Nondestructive Testing: A Training Guide", second edition, , John Wiley, United States, ISBN 978-0-471-42029-3, 2005
7. Boutin, G., Lupien, C. " Thermal Cracking of Asphalt Pavement", 2nd Eurasphalt & Eurobitumen Congress, Barcelona, 2000
8. Khosla, N.P., Goetz, W.H. "Tensile characteristics of bituminous mixtures as affected by modified binders", Association of Asphalt Paving Technologists, Vol. 48, pp.34-64, 1979.
9. Valkering. C.P., Jongeneel.D.J. "Acoustic Emission for evaluating the relative performance of asphalt mixes under thermal loading conditions," Association of Asphalt Paving Technologists, Vol. 60, pp.160-187, 1991.
10. Hesp. S.T., Terlouw, T., Vonk, W. "Low temperature performance of SBS-modified mixes," Association of Asphalt Paving Technologists, Vol. 69, pp.540-573, 2000.
11. Li, X., Marasteanu, M.O., Iverson, N., Labuz, J.F. "Observation of Crack Propagation in Asphalt Mixtures with acoustic emission," Transportation Research Record: Journal of the Transportation Research Board, No. 1970, Transportation Research Board of the National Academies, Washington, D.C., pp. 171–177, 2006

12. Nesvijski, E., Marasteanu, M. "Spectral Analysis of Acoustic Emission of Cold Cracking Asphalt," NDT.net, Vol. 11, No. 10, Sep 2006.
13. AASHTO TP1, "Standard specification for determining the flexural creep stiffness of asphalt binder using the bending beam rheometer (BBR)" American Association of State Highway and Transportation Officials, Washington, D.C., 1999.
14. Stuart, K.D., and Youtcheff, J.S., "Understanding the Performance of modified asphalt binders: low-temperature properties," Final Report FHWA-RD-02-074. FHWA, 2002.
15. Apeagyei, A.K., "Development of antioxidant treatment for asphalt binders and mixtures", Ph.D. Thesis, University of Illinois at Urbana-Champaign, 2005.
16. ASTM D 6521 – 05, "Accelerated Aging of Asphalt Binder Using a Pressurized Aging Vessel (PAV)" American Society for Testing and Materials, 2005.
17. AASHTO TP9-96. Standard Test Method for Determining the Creep Compliance and Strength of Hot Mix Asphalt (HMA) Using the Indirect Tensile Test Device.
18. Dave.E.V., Behnia, B., Ahmed, S., Buttlar, W.G., and Reis, H." Low Temperature Fracture Evaluation of Asphalt Mixtures using Mechanical Testing and Acoustic Emissions Techniques," Association of Asphalt Paving Technologists Journal, 2011 (Accepted)
19. Blankenship, P. Anderson, M., King, G., Hanson, D.I., "A Laboratory and Field Investigation to Develop Test Procedures for Predicting Non-Load Associated Cracking of Airfield HMA Pavements, Project 06-01 (Phase II) Final Report, August, 2010
20. Behnia, B., Dave.E.V., Ahmed, S., Buttlar, W.G., and Reis, H." Investigation of Effects of the Recycled Asphalt Pavement (RAP) Amounts on Low Temperature Cracking Performance of Asphalt Mixtures using Acoustic Emissions (AE)" , Journal of the Transportation Research Board, Washington D.C., 2011 (Accepted)
21. [http://en.wikipedia.org/wiki/Thermoelectric\\_cooling](http://en.wikipedia.org/wiki/Thermoelectric_cooling)
22. <http://arstechnica.com/guide/cooling/peltier-1.html>
23. [http://stirlingultracold.com/shuttle\\_home](http://stirlingultracold.com/shuttle_home)

## **LIST of PUBLICATIONS:**

### **JOURNAL PAPERS:**

1. Behnia, B., Dave.E.V., Ahmed, S., Buttlar, W.G., and Reis, H.” Investigation of Effects of the Recycled Asphalt Pavement (RAP) Amounts on Low Temperature Cracking Performance of Asphalt Mixtures using Acoustic Emissions (AE)” , Journal of the Transportation Research Board, No. 2208, Transportation Research Board of the National Academies, Washington, D.C., 2011, pp. 64–71
2. Dave.E.V., Behnia, B., Ahmed, S., Buttlar, W.G., and Reis, H.” Low Temperature Fracture Evaluation of Asphalt Mixtures using Mechanical Testing and Acoustic Emissions Techniques,” Journal of Association of Asphalt Paving Technologists, 2011 (In Press)
3. Hill, B., Behnia, B., Hakimzadeh, S., Buttlar, W.G., and Reis, H.” Evaluation of the Low Temperature Cracking Performance of WMA Mixtures,”, Journal of the Transportation Research Board, Transportation Research Board of the National Academies, Washington, D.C. (Accepted for publication).

### **CONFERENCE PAPERS:**

1. Behnia, B., Buttlar, W.G., Apeagyei, A.K., and Reis, H. .”Determining the embrittlement temperature of asphalt binders using an acoustic emission approach,” NDE/NDT for Highways and Bridges: Structural Materials Technology (SMT), New York, 2010